Modern Physics Letters A

IMPLEMENTATION OF THE CMS-SUS-19-006 ANALYSIS IN THE MadAnalysis 5 FRAMEWORK

Malte Mrowietz

Institut für Experimental Physik, Universität Hamburg, Luruper Chaussee 149 Hamburg, D-22671, Deutschland

Sam Bein

Institut für Experimental Physik, Universität Hamburg, Luruper Chaussee 149 Hamburg, D-22671, Deutschland

Jory Sonneveld

Institut für Experimental Physik, Universität Hamburg, Luruper Chaussee 149 Hamburg, D-22671, Deutschland

Received (Day Month Year)
Revised (Day Month Year)

We present the MadAnalysis 5 implementation and validation of the analysis *Search for supersymmetry in proton-proton collisions at 13 TeV in final states with jets and missing transverse momentum* (CMS-SUS-19-006). The search targets signatures with at least two jets and large missing transverse momentum in the all-hadronic final state. The analyzed luminosity is 137 fb^{-1}, corresponding to the Run 2 proton-proton data set recorded by the CMS detector at 13 TeV. This implementation has been validated in a variety of simplified models, by comparing derived cut flow tables and histograms with information provided by the CMS collaboration, using event samples that we simulated for the purpose of this re-implementation study. The validation is found to reproduce the signal acceptance in most cases.

1. Introduction

Proton-proton collisions (events) that feature significant hadronic activity in combination with large missing transverse momentum E_T^{miss} in the final state can act as a probe for a general class of beyond the Standard Model (BSM) models. In particular, models of R-parity conserving supersymmetry (SUSY) that feature TeV-scale squarks or gluinos often have these attributes as hallmark signal event characteristics. Therefore, the data analyzed in the all-hadronic multi-jet channel [1] provide an important constraint on generic dark matter models and strong-production SUSY.

A MadAnalysis 5[3–6] implementation of [1] has been carried out for the purpose of allowing for the reinterpretation of the results of this search in any new physics context.[7] This note provides supporting documentation for the implementation and details steps taken to validate the work using information made public by CMS. This

information pertains to the efficiency and acceptance of signal events of benchmark points within the simplified models of gluino pair production with decays of $\tilde{g} \to q\bar{q}\tilde{\chi}_1^0$, $\tilde{g} \to b\bar{b}\tilde{\chi}_1^0$, and $\tilde{g} \to b\bar{b}\tilde{\chi}_1^0$, denoted T1qqqq, T1tttt, T1bbbb, T5qqqqVV, respectively, as well as squark pair production featuring $\tilde{q} \to q\tilde{\chi}_1^0$, $\tilde{q} \to b\tilde{\chi}_1^0$, and $\tilde{t} \to q\tilde{\chi}_1^0$, denoted T2qq, T2tt, and T2bb, respectively.

2. Description of the analysis

The analysis defines 174 signal regions (SRs) that target a variety of final states. The region definitions are based on requirements on t$H_{\mathrm{T}}^{\mathrm{miss}}$, the transverse hadronic activity H_{T} , jet and b-jet multiplicity. Here, the missing transverse hadronic momentum $H_{\mathrm{T}}^{\mathrm{miss}}$ is used as a proxy for the E_T^{miss}. The lower multiplicity regions probe squark pair production models where large multiplicities are more sensitive to gluinos. Categories with large b-jet multiplicity help target scenarios with kinematically accessible third-generation squarks, while the 0-b bins increase sensitivity to first and second generation squark models. Larger and smaller $H_{\mathrm{T}}^{\mathrm{miss}}$ and H_{T} regions respectively target compressed and uncompressed mass spectra.

2.1. *Object definitions*

The primary objects used in the CMS analysis are particle flow jets, obtained by a clustering of all reconstructed particles with trajectories pointing to the primary vertex using the anti-k_{T}[8] jet algorithm with a cone size parameter of 0.4. Jets are required to have

- $p_{\mathrm{T}} > 30$ GeV and
- $|\eta| < 5.0$.

Because particle flow jets are the basis of the calculation of $E_{\mathrm{T}}^{\mathrm{miss}}$, they are inclusive with respect to all reconstructed energy in an event. To emulate this behavior in `Delphes`, we avoid the use of the `UniqueObjectFinder` module, and this is consistent with the detector card recommended as default in association with `MadAnalysis 5`.

Detector smearing of hadron energy is kept as default, and the jet energy scale (JES) applied by default in `Delphes` has been removed. Additionally, the jet cone size parameter for the anti-k_{T} algorithm used in `Delphes` has been changed from the default to R=0.4, as required in the paper. Finally, the cone size parameter for flavor assignment in the `Delphes` card has been changed to 0.4. The `MadAnalysis 5` interface to `Delphes` also removes jets which are identified as originating from τ lepton decays from the `Jet` collection. These jets are added back in to the jet collection in the implemented C++ analyzer code.

Leptons are identified if they point to the primary vertex, are isolated, and satisfy

- $p_{\mathrm{T}} >$10 GeV and

- $|\eta| < 2.5$ (2.4) for electrons (muons)
- $I < 0.1(0.2)$ for electrons (muons).

For the isolation I, we implement the so-called "mini" relative isolation definition, which for a lepton candidate i, is given by

- $(1/p_{Ti}) \sum_{j \neq i}^{n} p_{Tj} < 0.2$.

Here, the sum runs over all particles j with a cone of variable radius around the candidate lepton. The radius is given by

$$R^* = \begin{cases} 0.2 & : p_T \leq 50 \text{ GeV} \\ (10 \text{ GeV})/p_T & : 50 < p_T \leq 200 \text{ GeV} \\ 0.05 & : p_T > 200 \text{ GeV}. \end{cases}$$

Photons are identified if they have

- $p_{\mathrm{T}} >$100 GeV and
- $|\eta| < 2.5$,

and are relatively isolated based on a fixed cone size of 0.3. Note that the isolation criterion for photons is somewhat simplified compared to the paper, since the CMS isolation is performed for each component's contribution to the p_T sum, the components being: charged hadrons, neutral hadrons, and electromagnetic particles. The impact of the photon veto on signal efficiency is small or negligible for the interpreted models. The analysis also applies a veto based on the presence of isolated tracks which were not identified as a lepton, aimed at further suppressing backgrounds from W+Jets and $t\bar{t}$ processes. Slightly different object criteria are placed on isolated tracks attributed to electrons, muons, and pions, all together summarized as

- $p_{\mathrm{T}} >$5 GeV,
- $|\eta| < 2.4$,
- $m_{\mathrm{T}}(\text{track}, H_{\mathrm{T}}^{\mathrm{miss}}) < 100$ GeV, and
- $I < 0.2$ (0.1) for electron and muon (pion) tracks,

where I is the relative isolation taken with respect to other tracks within a constant-size cone of radius 0.3 around the candidate track.

2.2. *Event selection*

The baseline selection is as follows:

- $H_{\mathrm{T}}^{\mathrm{miss}} = |\vec{H}_{\mathrm{T}}^{\mathrm{miss}}| > 300$ GeV, where $\vec{H}_{\mathrm{T}}^{\mathrm{miss}}$ is the negative $\vec{p}_T$ sum of all selected jets;
- $H_{\mathrm{T}} > 300$ GeV, where H_{T} is the scalar sum of the p_{T} of jets within $|\eta| < 2.4$;
- $H_{\mathrm{T}} > H_{\mathrm{T}}^{\mathrm{miss}}$;

- $n_j > 1$, where n_j is the number of jets within $|\eta| < 2.4$;
- $n_e = n_\mu = n_\gamma = n_{\text{iso tracks}} = 0$;
- $\Delta\phi(\vec{j}_{1,2,3,4}, \vec{H}_{\text{T}}^{\text{miss}}) > 0.5, 0.5, 0.3, 0.3$, where $\{j_i\}$ is the p_{T}-ordered list of jets in a given event.

Our implementation accounts for cases in which long-lived charginos are reconstructed as muons, and thus trigger the muon event veto. This is done by treating any chargino with a decay length of > 3 m to be a muon.

Events passing the baseline selection are further categorized into orthogonal signal regions defined by ranges of $H_{\text{T}}^{\text{miss}}$, H_{T}, n_j, and n_b. The boundaries in the $H_T - H_T^{\text{miss}}$ plane are shown in Fig. 1. Each region is further split into categories based on n_{jets} of [2,3], [4,5], [6,8],[8,10],$>$ 10, and $n_{b-\text{tags}} = 0, 1, 2, \geq 3$, and the complete list of signal regions is given in Tables 3-7 of [1]. It is noted that the search bins correspond to the regions 1 and 4 in Fig. 1 are dropped for N ≥ 8.

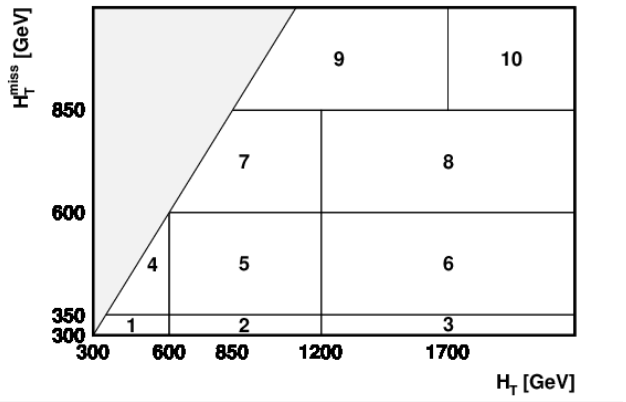

Fig. 1. Boundaries in the $H_T - H_T^{\text{miss}}$ plane which go into defining the final search bins [1].

An alternative, smaller set of aggregate signal regions, totaling 12 in number, is also defined in Table 9 of [1]. The former SR's are mutually exclusive event categories and thus can be more safely used in a combination analysis, whereas the latter aggregate regions have significant overlaps in phase space. Each aggregate region has been defined in a way to give reasonably good sensitivity to a particular type of signal model. For example, Aggregate Bin 11, which requires H_T and $H_T^{\text{miss}} >$ 600 GeV, > 5 jets, and at least 1 b-tagged jet, should provide good sensitivity to models with top squark production, particularly in uncompressed mass regimes. By contrast, Bin 1 is more inclusive and may be most suitable for probing generic 1st generation squark or dark matter production, given that it is more inclusive and that it vetoes events with one or more b-jets. In some cases, the use of a likelihood based on a single aggregate bin, e.g., that giving the largest expected significance,

can be a good choice for establishing constraints on a model. The the most sensitive approach is to use a combination of several or even all 174 bins in a likelihood. CMS has provided covariance and correlation matrixes for the regions, which can be utilized for this purpose.

The provided analysis code produces an estimate of the signal acceptance calculation for all 174 signal regions, as well as the aggregated signal regions.

3. Validation

We validate the implementation based on cut flow tables and distributions of kinematic observables provided by the analysis in its public webspace.[2] The needed event samples as well as the results of the validation are described in the following.

3.1. *Event samples*

Simulated event samples have been prepared for a host of benchmark signal model scenarios, corresponding to the simplified models specified in the introduction. For each model one compressed and one uncompressed scenario has been examined. The event generation has been carried out using `MadGraph5_aMC@NLO` version 2.7.2,[9] making use of the UFO[10] file `MSSM_SLHA2`[11] and relying on matrix elements including up to three additional partonic jet constituents. The parton distribution function (PDF) used is `NNPDF23_nlo_as_0119` [12] as implemented with `LHAPDF`.[13] Gluino and squark decays are implemented in Pythia8 [14,15,15], as well as parton showering and hadronization. Jet merging is iwith implemented with an `xqcut` value of 30 GeV and `qcut` parameter values ranging from 68 to 171 according to the mother particle mass. For additional information, equivalent event samples have been generated and hadronized (full chain) using leading order (LO) `Pythia8`. In all cases the `Delphes` implementation with a lightly modified detector card has been used to simulate the response of the CMS detector to these events. The modifications include the inclusion of the CMS b-tagging efficiency parameterization for the *deepCSV* flavor algorithm, provided in [16]. The medium working point efficiency has been used, as that is what is used by the analysis. This parameterization has been modified by removing the quadratic term from the $p_T > 250\,\text{GeV}$ part and approximating with a constant efficiency for $p_T > 1300\,\text{GeV}$. The main reason for this is that the parameterization is not defined for $p_T > 1000$, and the functional form with the quadratic term gains a positive slope above 1000 GeV, which is not physical. The fact that the efficiency continues to decrease for high-p_T is evidenced by our overprediction of n_b for uncompressed bottom squark models. The original, rounded to two significant digits, is

$$\epsilon = \begin{cases} (20,50]: & .19 + .021p_T - .00035p_T^2 + 2.8\cdot 10^{-6}p_T^3 - 1.0\cdot 10^{-8}p_T^4 + 1.5\cdot 10^{-11}p_T^5 \\ (50,250]: & .56 + .0034p_T - 3.3\cdot 10^{-5}p_T^2 + 1.5\cdot 10^{-7}p_T^3 - 3.6\cdot 10^{-10}p_T^4 + 3.5\cdot 10^{-13}p_T^5 \\ > 250: & .77 - .00055p_T + 2.9\cdot 10^{-7}p_T^2. \end{cases}$$

where the ranges are given for p_T in units of GeV. We have dropped the last term, and seen that this change leads to a 15% improvement in the highest and lowest b-tag mulitiplicity regions for the models T1bbbb and T2bb, and has minimal effect on other models.

3.2. *Comparison with the official results*

This section compares results derived from the recast implementation with the official results from CMS. A table showing a comparison of the cut efficiencies is given for each model, along with the signal event count in each aggregate signal region. Additionally, distributions of kinematic observables used to define the signal regions are compared after the application of the baseline event selection. The degree of validation of the recast implementation is reflected in the comparison between the `MadGraph5_aMC@NLO` and the CMS result. The result obtained from LO `Pythia8` is provided for reference.

A generally satisfactory agreement is seen between the recast implementation and official versions, with a few exceptions. Particularly, there is a logical inconsistency in the aggregate signal region counts for the model T1qqqq(1300,100), where the numbers indicate the mother particle and LSP mass in GeV. We have reported these anomalies to the CMS team and they are working to fix it. However, we think this only impacts the validation material for these models, and does not undermine this implementation.

Minor trends and disagreements come into the picture when considering models that produce heavy flavor jets. Particularly, models with real or virtual bottom squarks exhibit a slight bias toward larger b-tagged jet multiplicities, while the opposite is true for events with top squarks. This effect is most notable in the uncompressed mass regimes. We have conducted numerous tests to investigate the source of this discrepancy, including making adjustments to the `Delphes` b-tagging efficiency, the jet energy scale, the way in which true b-jets are defined at the level of the generator, as well as changes to the PDF used in the `MadGraph5_aMC@NLO` generation. We find that the choice of PDF has the most pronounced impact on the distribution of b-tagged jet multiplicity than any other change, which lead to difference with respect to CMS. However, our final validation is based on the `LHAPDF` implementation consistent with that described by the analysis, and in the case of compressed 3rd generation squark models, a slight over-prediction in b-tagged jet multiplicity is observed. We think this is due to inefficiencies that arise from excess transverse event activity, which are not captured by the efficiencies reported by CMS.

In a handful of cases, larger discrepancies of order 50% appear in the count comparisons in the signal regions, but these are typically within the statistical uncertainties in the signal counts. In rare cases, there is no predicted value for the signal in a given aggregate signal region. This should not have an unwanted effect on limit setting because such bins are not typically sensitive to models with

nearly negligible yield, and the inclusion of such bins will not impact the likelihood.

Table 1. Pre-selection cutflow for the T1qqqq-1300-100 simplified model.

Cut	MA5 Pythia8	MA5 Madgraph5 +Pythia8	CMS	MA5 Pythia8 diff [%]	MA5 Madgraph5 +Pythia8 diff [%]	MA5 Pythia8 drop [%]	MA5 Madgraph5 +Pythia8 drop [%]	CMS drop [%]
$N_{jet} \geq 2$	$100.0\pm^{0.0}_{0.0}$	$100.0\pm^{0.0}_{0.1}$	100.0±0.0	0.0	0.0	0.0	0.0	0.0
$H_T > 300$	$100.0\pm^{0.0}_{0.0}$	$100.0\pm^{0.0}_{0.1}$	100.0±0.0	0.0	0.0	0.0	0.0	0.0
$H_T^{miss} > 300$	$67.5\pm^{0.5}_{0.5}$	$75.3\pm^{0.9}_{0.9}$	77.1±0.5	12.45	2.33	32.5	24.7	22.9
$H_T > H_T^{miss}$	$67.3\pm^{0.5}_{0.5}$	$75.2\pm^{0.9}_{0.9}$	77.0±0.5	12.6	2.34	0.2	0.1	0.1
NoIsoMuons	$67.3\pm^{0.5}_{0.5}$	$75.1\pm^{0.9}_{0.9}$	76.9±0.5	12.48	2.34	0.0	0.1	0.1
NoMuonsTracks	$67.2\pm^{0.5}_{0.5}$	$75.1\pm^{0.9}_{0.9}$	76.8±0.5	12.5	2.21	0.1	0.0	0.1
NoIsoElectrons	$67.2\pm^{0.5}_{0.5}$	$75.0\pm^{0.9}_{0.9}$	76.5±0.5	12.16	1.96	0.0	0.1	0.3
NoElectronsTracks	$67.1\pm^{0.5}_{0.5}$	$75.0\pm^{0.9}_{0.9}$	76.1±0.5	11.83	1.45	0.1	0.0	0.4
NoIsoTracks	$66.7\pm^{0.5}_{0.5}$	$74.5\pm^{0.9}_{0.9}$	75.3±0.5	11.42	1.06	0.4	0.5	0.8
NoIsoPhotons	$65.7\pm^{0.5}_{0.5}$	$73.4\pm^{0.9}_{1.0}$	72.5±0.5	9.38	-1.24	1.0	1.1	2.8
$\Delta\Phi_{H_T^{miss},j1} > 0.5$	$64.9\pm^{0.5}_{0.5}$	$72.2\pm^{1.0}_{1.0}$	71.2±0.5	8.85	-1.4	0.8	1.2	1.3
$\Delta\Phi_{H_T^{miss},j2} > 0.5$	$58.7\pm^{0.5}_{0.5}$	$65.6\pm^{1.0}_{1.0}$	64.5±0.6	8.99	-1.71	6.2	6.6	6.7
$\Delta\Phi_{H_T^{miss},j3} > 0.3$	$54.7\pm^{0.5}_{0.5}$	$60.7\pm^{1.0}_{1.1}$	59.6±0.6	8.22	-1.85	4.0	4.9	4.9
$\Delta\Phi_{H_T^{miss},j4} > 0.3$	$50.4\pm^{0.5}_{0.5}$	$55.6\pm^{1.1}_{1.1}$	54.9±0.6	8.2	-1.28	4.3	5.1	4.7

Table 2. Signal yield in the aggregated signal regions for the T1qqqq-1300-100 simplified model.

Agg SR	MA5 Pythia8 yield	MA5 Madgraph5+Pythia8 yield	CMS yield	MA5 Pythia8 diff [%]	MA5 Madgraph5+Pythia8 diff [%]
SR1 $N_{jet} \geq 2$ $N_{bjet} = 0$ $H_T > 600$ $H_T^{miss} > 600$	989.86±25.93	1335.46±63.17	121.16±1.14	-716.99	-1002.23
SR2 $N_{jet} \geq 4$ $N_{bjet} = 0$ $H_T > 1700$ $H_T^{miss} > 850$	91.72±7.89	206.15±24.82	57.3±0.78	-60.07	-259.77
SR3 $N_{jet} \geq 6$ $N_{bjet} = 0$ $H_T > 600$ $H_T^{miss} > 600$	467.42±17.82	717.03±46.28	60.23±0.76	-676.06	-1090.49
SR4 $N_{jet} \geq 8$ $N_{bjet} = 0-1$ $H_T > 600$ $H_T^{miss} > 600$	131.8±9.46	247.97±27.22	21.9±0.39	-501.83	-1032.28
SR5 $N_{jet} \geq 10$ $N_{bjet} = 0-1$ $H_T > 1700$ $H_T^{miss} > 850$	5.44±1.92	5.98±4.23	1.96±0.1	-177.55	-205.1
SR6 $N_{jet} \geq 4$ $N_{bjet} \geq 2$ $H_T > 300$ $H_T^{miss} > 300$	95.79±8.07	125.48±19.36	7.41±0.11	-1192.71	-1593.39
SR7 $N_{jet} \geq 2$ $N_{bjet} \geq 2$ $H_T > 600$ $H_T^{miss} > 600$	33.97±4.8	47.8±11.95	5.01±0.09	-578.04	-854.09
SR8 $N_{jet} \geq 6$ $N_{bjet} \geq 2$ $H_T > 350$ $H_T^{miss} > 350$	54.35±6.08	62.74±13.69	5.26±0.1	-933.27	-1092.78
SR9 $N_{jet} \geq 4$ $N_{bjet} \geq 2$ $H_T > 600$ $H_T^{miss} > 600$	33.97±4.8	44.81±11.57	4.97±0.09	-583.5	-801.61
SR10 $N_{jet} \geq 8$ $N_{bjet} \geq 3$ $H_T > 300$ $H_T^{miss} > 300$	3.4±1.52	8.96±5.17	0.37±0.02	-818.92	-2321.62
SR11 $N_{jet} \geq 6$ $N_{bjet} \geq 1$ $H_T > 600$ $H_T^{miss} > 600$	120.93±9.06	149.38±21.13	21.88±0.27	-452.7	-582.72
SR12 $N_{jet} \geq 10$ $N_{bjet} \geq 3$ $H_T > 850$ $H_T^{miss} > 850$	0.0±0.0	0.0±0.0	0.03±0.01	100.0	100.0

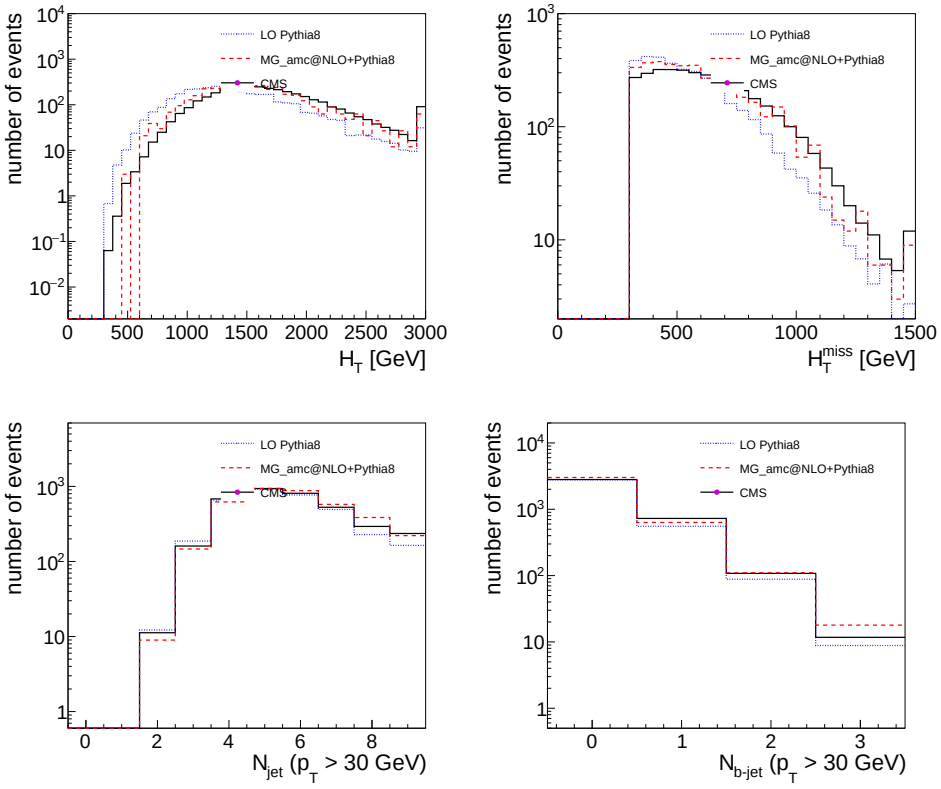

Fig. 2. Kinematic distributions for the T1qqqq-1300-100 simplified model for the madanalysis5 implementation and those provided by CMS

Table 3. Pre-selection cutflow for the T1qqqq-1200-1000 simplified model.

Cut	MA5 Pythia8	MA5 Madgraph5 +Pythia8	CMS	MA5 Pythia8 diff [%]	MA5 Madgraph5 +Pythia8 diff [%]	MA5 Pythia8 drop [%]	MA5 Madgraph5 +Pythia8 drop [%]	CMS drop [%]
$N_{jet} \geq 2$	$93.0\pm^{0.3}_{0.3}$	$99.5\pm^{0.1}_{0.2}$	99.6±0.1	6.63	0.1	7.0	0.5	0.4
$H_T > 300$	$67.7\pm^{0.5}_{0.5}$	$79.8\pm^{0.9}_{0.9}$	82.0±0.3	17.44	2.68	25.3	19.7	17.6
$H_T^{miss} > 300$	$30.0\pm^{0.5}_{0.5}$	$20.8\pm^{0.9}_{0.9}$	21.2±0.4	-41.51	1.89	37.7	59.0	60.8
$H_T > H_T^{miss}$	$29.5\pm^{0.5}_{0.5}$	$20.7\pm^{0.9}_{0.9}$	20.9±0.4	-41.15	0.96	0.5	0.1	0.3
NoIsoMuons	$29.5\pm^{0.5}_{0.5}$	$20.7\pm^{0.9}_{0.9}$	20.8±0.4	-41.83	0.48	0.0	0.0	0.1
NoMuonsTracks	$29.5\pm^{0.5}_{0.5}$	$20.7\pm^{0.9}_{0.9}$	20.8±0.4	-41.83	0.48	0.0	0.0	0.0
NoIsoElectrons	$29.4\pm^{0.5}_{0.5}$	$20.7\pm^{0.9}_{0.9}$	20.7±0.4	-42.03	0.0	0.1	0.0	0.1
NoElectronsTracks	$29.4\pm^{0.5}_{0.5}$	$20.7\pm^{0.9}_{0.9}$	20.6±0.4	-42.72	-0.49	0.0	0.0	0.1
NoIsoTracks	$29.0\pm^{0.5}_{0.5}$	$20.4\pm^{0.9}_{0.9}$	20.1±0.4	-44.28	-1.49	0.4	0.3	0.5
NoIsoPhotons	$28.8\pm^{0.5}_{0.5}$	$20.0\pm^{0.9}_{0.9}$	19.5±0.3	-47.69	-2.56	0.2	0.4	0.6
$\Delta\Phi_{H_T^{miss},j1} > 0.5$	$28.7\pm^{0.5}_{0.5}$	$20.0\pm^{0.9}_{0.9}$	19.5±0.3	-47.18	-2.56	0.1	0.0	0.0
$\Delta\Phi_{H_T^{miss},j2} > 0.5$	$26.7\pm^{0.4}_{0.4}$	$18.5\pm^{0.9}_{0.8}$	17.9±0.3	-49.16	-3.35	2.0	1.5	1.6
$\Delta\Phi_{H_T^{miss},j3} > 0.3$	$25.1\pm^{0.4}_{0.4}$	$17.5\pm^{0.9}_{0.8}$	16.9±0.3	-48.52	-3.55	1.6	1.0	1.0
$\Delta\Phi_{H_T^{miss},j4} > 0.3$	$23.6\pm^{0.4}_{0.4}$	$16.7\pm^{0.8}_{0.8}$	15.9±0.3	-48.43	-5.03	1.5	0.8	1.0

Table 4. Signal yield in the aggregated signal regions for the T1qqqq-1200-1000 simplified model.

Agg SR	MA5 Pythia8 yield	MA5 Madgraph5+Pythia8 yield	CMS yield	MA5 Pythia8 diff [%]	MA5 Madgraph5+Pythia8 diff [%]
SR1 $N_{jet} \geq 2$ $N_{bjet} = 0$ $H_T > 600$ $H_T^{miss} > 600$	448.69±23.98	312.53±42.93	193.14±3.02	-132.31	-61.82
SR2 $N_{jet} \geq 4$ $N_{bjet} = 0$ $H_T > 1700$ $H_T^{miss} > 850$	19.23±4.97	11.79±8.34	13.84±0.76	-38.95	14.81
SR3 $N_{jet} \geq 6$ $N_{bjet} = 0$ $H_T > 600$ $H_T^{miss} > 600$	182.04±15.28	147.42±29.48	111.28±2.16	-63.59	-32.48
SR4 $N_{jet} \geq 8$ $N_{bjet} = 0-1$ $H_T > 600$ $H_T^{miss} > 600$	52.56±8.21	76.66±21.26	46.1±1.18	-14.01	-66.29
SR5 $N_{jet} \geq 10$ $N_{bjet} = 0-1$ $H_T > 1700$ $H_T^{miss} > 850$	1.28±1.28	5.9±5.9	1.53±0.19	16.34	-285.62
SR6 $N_{jet} \geq 4$ $N_{bjet} \geq 2$ $H_T > 300$ $H_T^{miss} > 300$	46.15±7.69	58.97±18.65	44.8±0.54	-3.01	-31.63
SR7 $N_{jet} \geq 2$ $N_{bjet} \geq 2$ $H_T > 600$ $H_T^{miss} > 600$	8.97±3.39	23.59±11.79	8.58±0.24	-4.55	-174.94
SR8 $N_{jet} \geq 6$ $N_{bjet} \geq 2$ $H_T > 350$ $H_T^{miss} > 350$	20.51±5.13	47.17±16.68	24.44±0.41	16.08	-93.0
SR9 $N_{jet} \geq 4$ $N_{bjet} \geq 2$ $H_T > 600$ $H_T^{miss} > 600$	8.97±3.39	23.59±11.79	8.48±0.24	-5.78	-178.18
SR10 $N_{jet} \geq 8$ $N_{bjet} \geq 3$ $H_T > 300$ $H_T^{miss} > 300$	0.0±0.0	5.9±5.9	1.59±0.08	100.0	-271.07
SR11 $N_{jet} \geq 6$ $N_{bjet} \geq 1$ $H_T > 600$ $H_T^{miss} > 600$	30.77±6.28	53.07±17.69	40.23±0.76	23.51	-31.92
SR12 $N_{jet} \geq 10$ $N_{bjet} \geq 3$ $H_T > 850$ $H_T^{miss} > 850$	0.0±0.0	0.0±0.0	0.07±0.02	100.0	100.0

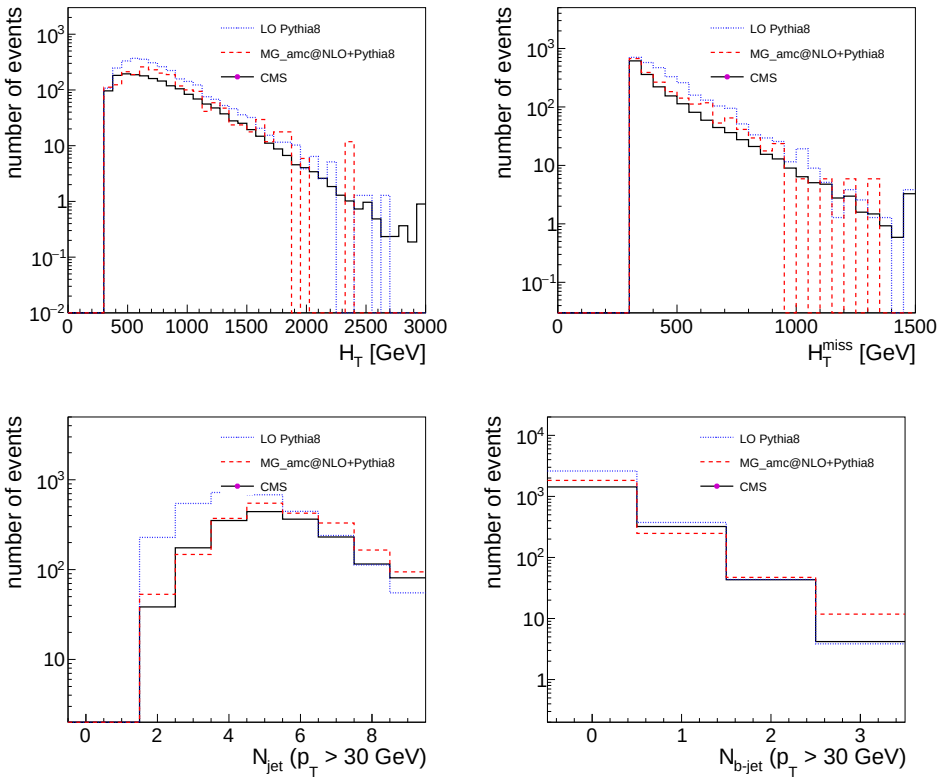

Fig. 3. Kinematic distributions for the T1qqqq-1200-1000 simplified model for the madanalysis5 implementation and those provided by CMS

Table 5. Pre-selection cutflow for the T1bbbb-1300-1100 simplified model.

Cut	MA5 Pythia8	MA5 Madgraph5 +Pythia8	CMS	MA5 Pythia8 diff [%]	MA5 Madgraph5 +Pythia8 diff [%]	MA5 Pythia8 drop [%]	MA5 Madgraph5 +Pythia8 drop [%]	CMS drop [%]
$N_{jet} \geq 2$	$93.3\pm^{0.2}_{0.3}$	$99.6\pm^{0.1}_{0.2}$	99.3±0.1	6.04	-0.3	6.7	0.4	0.7
$H_T > 300$	$68.3\pm^{0.5}_{0.5}$	$74.8\pm^{0.9}_{0.9}$	74.8±0.5	8.69	0.0	25.0	24.8	24.5
$H_T^{miss} > 300$	$30.9\pm^{0.5}_{0.5}$	$20.0\pm^{0.9}_{0.8}$	19.9±0.5	-55.28	-0.5	37.4	54.8	54.9
$H_T > H_T^{miss}$	$30.6\pm^{0.5}_{0.5}$	$19.7\pm^{0.9}_{0.8}$	19.5±0.5	-56.92	-1.03	0.3	0.3	0.4
NoIsoMuons	$30.3\pm^{0.5}_{0.5}$	$19.7\pm^{0.9}_{0.8}$	19.2±0.5	-57.81	-2.6	0.3	0.0	0.3
NoMuonsTracks	$29.9\pm^{0.5}_{0.5}$	$19.5\pm^{0.9}_{0.8}$	18.9±0.5	-58.2	-3.17	0.4	0.2	0.3
NoIsoElectrons	$29.8\pm^{0.5}_{0.5}$	$19.4\pm^{0.9}_{0.8}$	18.8±0.5	-58.51	-3.19	0.1	0.1	0.1
NoElectronsTracks	$29.4\pm^{0.5}_{0.5}$	$19.2\pm^{0.9}_{0.8}$	18.4±0.5	-59.78	-4.35	0.4	0.2	0.4
NoIsoTracks	$29.2\pm^{0.5}_{0.5}$	$19.1\pm^{0.9}_{0.8}$	18.2±0.5	-60.44	-4.95	0.2	0.1	0.2
NoIsoPhotons	$29.1\pm^{0.5}_{0.5}$	$19.0\pm^{0.9}_{0.8}$	17.8±0.5	-63.48	-6.74	0.1	0.1	0.4
$\Delta\Phi_{H_T^{miss},j1} > 0.5$	$29.1\pm^{0.5}_{0.5}$	$19.0\pm^{0.9}_{0.8}$	17.7±0.5	-64.41	-7.34	0.0	0.0	0.1
$\Delta\Phi_{H_T^{miss},j2} > 0.5$	$27.2\pm^{0.5}_{0.4}$	$17.0\pm^{0.8}_{0.8}$	16.2±0.4	-67.9	-4.94	1.9	2.0	1.5
$\Delta\Phi_{H_T^{miss},j3} > 0.3$	$25.7\pm^{0.4}_{0.4}$	$16.0\pm^{0.8}_{0.8}$	15.1±0.4	-70.2	-5.96	1.5	1.0	1.1
$\Delta\Phi_{H_T^{miss},j4} > 0.3$	$24.1\pm^{0.4}_{0.4}$	$15.3\pm^{0.8}_{0.8}$	14.2±0.4	-69.72	-7.75	1.6	0.7	0.9

Table 6. Signal yield in the aggregated signal regions for the T1bbbb-1300-1100 simplified model.

Agg SR	MA5 Pythia8 yield	MA5 Madgraph5+Pythia8 yield	CMS yield	MA5 Pythia8 diff [%]	MA5 Madgraph5+Pythia8 diff [%]
SR1 $N_{jet} \geq 2$ $N_{bjet} = 0$ $H_T > 600$ $H_T^{miss} > 600$	37.37±5.04	14.69±6.57	4.85±0.19	-670.52	-202.89
SR2 $N_{jet} \geq 4$ $N_{bjet} = 0$ $H_T > 1700$ $H_T^{miss} > 850$	1.36±0.96	0.0±0.0	0.32±0.03	-325.0	100.0
SR3 $N_{jet} \geq 6$ $N_{bjet} = 0$ $H_T > 600$ $H_T^{miss} > 600$	8.83±2.45	5.87±4.15	1.68±0.08	-425.6	-249.4
SR4 $N_{jet} \geq 8$ $N_{bjet} = 0-1$ $H_T > 600$ $H_T^{miss} > 600$	5.44±1.92	14.69±6.57	3.21±0.15	-69.47	-357.63
SR5 $N_{jet} \geq 10$ $N_{bjet} = 0-1$ $H_T > 1700$ $H_T^{miss} > 850$	0.0±0.0	0.0±0.0	0.1±0.02	100.0	100.0
SR6 $N_{jet} \geq 4$ $N_{bjet} \geq 2$ $H_T > 300$ $H_T^{miss} > 300$	864.85±24.24	728.43±46.26	589.39±4.54	-46.74	-23.59
SR7 $N_{jet} \geq 2$ $N_{bjet} \geq 2$ $H_T > 600$ $H_T^{miss} > 600$	186.15±11.25	146.86±20.77	105.43±1.68	-76.56	-39.3
SR8 $N_{jet} \geq 6$ $N_{bjet} \geq 2$ $H_T > 350$ $H_T^{miss} > 350$	298.93±14.25	305.47±29.95	236.98±2.48	-26.14	-28.9
SR9 $N_{jet} \geq 4$ $N_{bjet} \geq 2$ $H_T > 600$ $H_T^{miss} > 600$	172.56±10.83	140.99±20.35	102.58±1.65	-68.22	-37.44
SR10 $N_{jet} \geq 8$ $N_{bjet} \geq 3$ $H_T > 300$ $H_T^{miss} > 300$	46.88±5.64	64.62±13.78	51.73±1.23	9.38	-24.92
SR11 $N_{jet} \geq 6$ $N_{bjet} \geq 1$ $H_T > 600$ $H_T^{miss} > 600$	116.85±8.91	96.93±16.87	76.83±1.33	-52.09	-26.16
SR12 $N_{jet} \geq 10$ $N_{bjet} \geq 3$ $H_T > 850$ $H_T^{miss} > 850$	2.04±1.18	0.0±0.0	1.07±0.16	-90.65	100.0

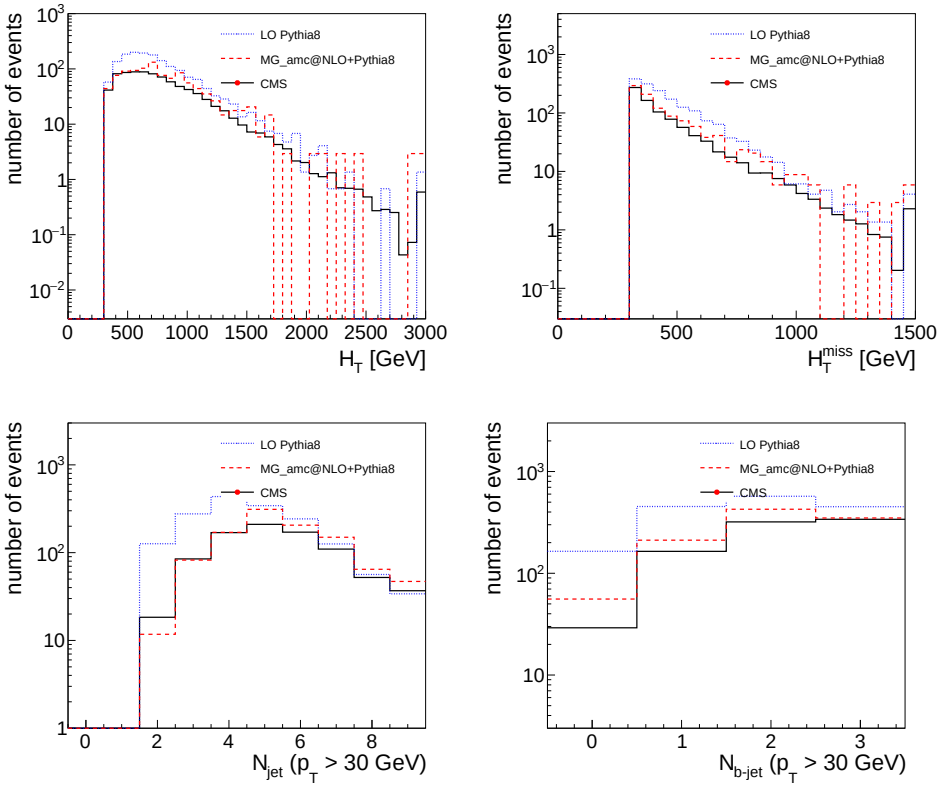

Fig. 4. Kinematic distributions for the T1bbbb-1300-1100 simplified model for the madanalysis5 implementation and those provided by CMS

Table 7. Pre-selection cutflow for the T1bbbb-1800-200 simplified model.

Cut	MA5 Pythia8	MA5 Madgraph5 +Pythia8	CMS	MA5 Pythia8 diff [%]	MA5 Madgraph5 +Pythia8 diff [%]	MA5 Pythia8 drop [%]	MA5 Madgraph5 +Pythia8 drop [%]	CMS drop [%]
$N_{jet} \geq 2$	$100.0\pm^{0.0}_{0.0}$	$100.0\pm^{0.0}_{0.1}$	100.0±0.5	0.0	0.0	0.0	0.0	0.0
$H_T > 300$	$100.0\pm^{0.0}_{0.0}$	$100.0\pm^{0.0}_{0.1}$	100.0±0.5	0.0	0.0	0.0	0.0	0.0
$H_T^{miss} > 300$	$80.2\pm^{0.4}_{0.4}$	$83.9\pm^{0.8}_{0.8}$	86.8±1.9	7.6	3.34	19.8	16.1	13.2
$H_T > H_T^{miss}$	$80.2\pm^{0.4}_{0.4}$	$83.8\pm^{0.8}_{0.8}$	86.8±1.9	7.6	3.46	0.0	0.1	0.0
NoIsoMuons	$79.9\pm^{0.4}_{0.4}$	$83.6\pm^{0.8}_{0.8}$	86.0±2.0	7.09	2.79	0.3	0.2	0.8
NoMuonsTracks	$79.8\pm^{0.4}_{0.4}$	$83.6\pm^{0.8}_{0.8}$	85.8±2.0	6.99	2.56	0.1	0.0	0.2
NoIsoElectrons	$79.6\pm^{0.4}_{0.4}$	$83.5\pm^{0.8}_{0.8}$	85.3±2.0	6.68	2.11	0.2	0.1	0.5
NoElectronsTracks	$79.5\pm^{0.4}_{0.4}$	$83.3\pm^{0.8}_{0.8}$	85.0±2.0	6.47	2.0	0.1	0.2	0.3
NoIsoTracks	$79.1\pm^{0.4}_{0.4}$	$83.0\pm^{0.8}_{0.8}$	84.3±2.0	6.17	1.54	0.4	0.3	0.7
NoIsoPhotons	$78.6\pm^{0.4}_{0.4}$	$82.3\pm^{0.8}_{0.8}$	81.5±2.1	3.56	-0.98	0.5	0.7	2.8
$\Delta\Phi_{H_T^{miss},j1} > 0.5$	$77.4\pm^{0.4}_{0.4}$	$80.5\pm^{0.8}_{0.8}$	80.0±2.2	3.25	-0.63	1.2	1.8	1.5
$\Delta\Phi_{H_T^{miss},j2} > 0.5$	$70.1\pm^{0.5}_{0.5}$	$74.1\pm^{0.9}_{0.9}$	71.8±2.4	2.37	-3.2	7.3	6.4	8.2
$\Delta\Phi_{H_T^{miss},j3} > 0.3$	$64.4\pm^{0.5}_{0.5}$	$68.1\pm^{1.0}_{1.0}$	66.6±2.5	3.3	-2.25	5.7	6.0	5.2
$\Delta\Phi_{H_T^{miss},j4} > 0.3$	$59.4\pm^{0.5}_{0.5}$	$62.4\pm^{1.0}_{1.0}$	61.1±2.6	2.78	-2.13	5.0	5.7	5.5

Table 8. Signal yield in the aggregated signal regions for the T1bbbb-1800-200 simplified model.

Agg SR	MA5 Pythia8 yield	MA5 Madgraph5+Pythia8 yield	CMS yield	MA5 Pythia8 diff [%]	MA5 Madgraph5+Pythia8 diff [%]
SR1 $N_{jet} \geq 2$ $N_{bjet} = 0$ $H_T > 600$ $H_T^{miss} > 600$	4.96±0.43	5.0±0.88	11.88±0.15	58.25	57.91
SR2 $N_{jet} \geq 4$ $N_{bjet} = 0$ $H_T > 1700$ $H_T^{miss} > 850$	1.14±0.21	2.5±0.62	4.95±0.1	76.97	49.49
SR3 $N_{jet} \geq 6$ $N_{bjet} = 0$ $H_T > 600$ $H_T^{miss} > 600$	1.6±0.25	1.72±0.52	4.77±0.08	66.46	63.94
SR4 $N_{jet} \geq 8$ $N_{bjet} = 0-1$ $H_T > 600$ $H_T^{miss} > 600$	2.52±0.31	3.44±0.73	5.68±0.12	55.63	39.44
SR5 $N_{jet} \geq 10$ $N_{bjet} = 0-1$ $H_T > 1700$ $H_T^{miss} > 850$	0.11±0.07	0.78±0.35	0.43±0.03	74.42	-81.4
SR6 $N_{jet} \geq 4$ $N_{bjet} \geq 2$ $H_T > 300$ $H_T^{miss} > 300$	169.58±2.54	175.05±5.23	143.99±0.82	-17.77	-21.57
SR7 $N_{jet} \geq 2$ $N_{bjet} \geq 2$ $H_T > 600$ $H_T^{miss} > 600$	94.92±1.9	120.55±4.34	100.49±0.69	5.54	-19.96
SR8 $N_{jet} \geq 6$ $N_{bjet} \geq 2$ $H_T > 350$ $H_T^{miss} > 350$	86.72±1.82	98.85±3.93	79.3±0.6	-9.36	-24.65
SR9 $N_{jet} \geq 4$ $N_{bjet} \geq 2$ $H_T > 600$ $H_T^{miss} > 600$	92.02±1.87	118.06±4.29	97.83±0.67	5.94	-20.68
SR10 $N_{jet} \geq 8$ $N_{bjet} \geq 3$ $H_T > 300$ $H_T^{miss} > 300$	16.89±0.8	21.39±1.83	12.97±0.26	-30.22	-64.92
SR11 $N_{jet} \geq 6$ $N_{bjet} \geq 1$ $H_T > 600$ $H_T^{miss} > 600$	59.68±1.51	82.76±3.6	74.87±0.57	20.29	-10.54
SR12 $N_{jet} \geq 10$ $N_{bjet} \geq 3$ $H_T > 850$ $H_T^{miss} > 850$	0.57±0.15	0.62±0.31	0.86±0.06	33.72	27.91

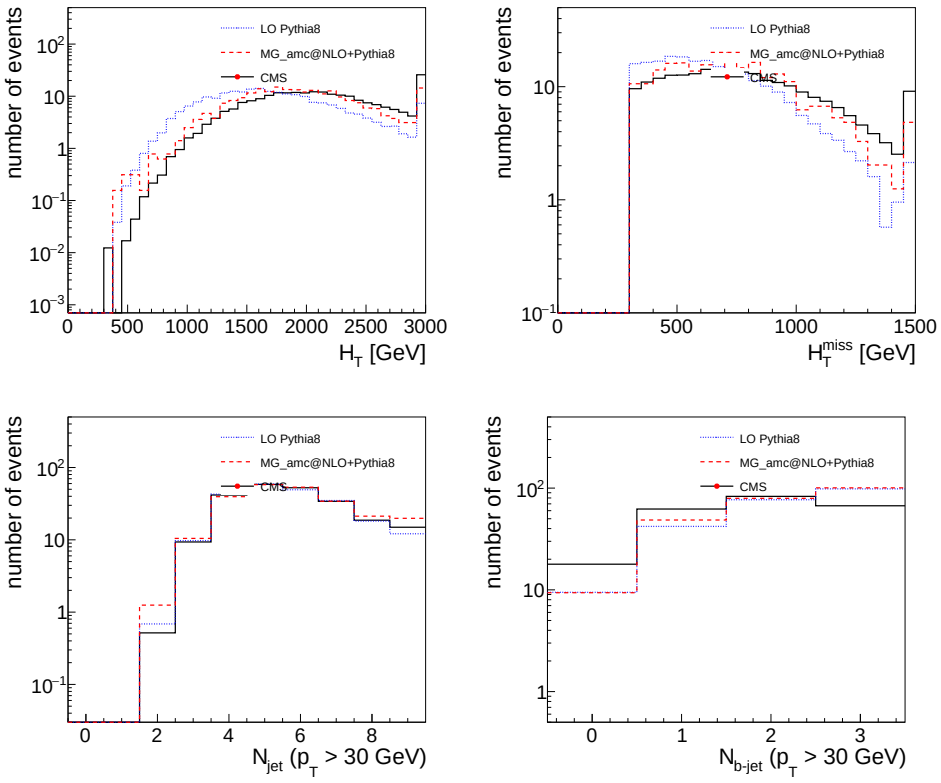

Fig. 5. Kinematic distributions for the T1bbbb-1800-200 simplified model for the madanalysis5 implementation and those provided by CMS

Table 9. Pre-selection cutflow for the T1tttt-1900-200 simplified model.

Cut	MA5 Pythia8	MA5 Madgraph5 +Pythia8	CMS	MA5 Pythia8 diff [%]	MA5 Madgraph5 +Pythia8 diff [%]	MA5 Pythia8 drop [%]	MA5 Madgraph5 +Pythia8 drop [%]	CMS drop [%]
$N_{jet} \geq 2$	$100.0\pm^{0.0}_{0.0}$	$100.0\pm^{0.0}_{0.1}$	100.0±0.8	0.0	0.0	0.0	0.0	0.0
$H_T > 300$	$100.0\pm^{0.0}_{0.0}$	$100.0\pm^{0.0}_{0.1}$	100.0±0.8	0.0	0.0	0.0	0.0	0.0
$H_T^{miss} > 300$	$77.4\pm^{0.4}_{0.4}$	$84.6\pm^{0.7}_{0.8}$	85.5±2.7	9.47	1.05	22.6	15.4	14.5
$H_T > H_T^{miss}$	$77.4\pm^{0.4}_{0.4}$	$84.5\pm^{0.7}_{0.8}$	85.5±2.7	9.47	1.17	0.0	0.1	0.0
NoIsoMuons	$50.2\pm^{0.5}_{0.5}$	$56.9\pm^{1.0}_{1.0}$	53.4±3.6	5.99	-6.55	27.2	27.6	32.1
NoMuonsTracks	$49.7\pm^{0.5}_{0.5}$	$56.4\pm^{1.0}_{1.0}$	52.6±3.6	5.51	-7.22	0.5	0.5	0.8
NoIsoElectrons	$33.1\pm^{0.5}_{0.5}$	$38.0\pm^{1.0}_{1.0}$	34.2±3.4	3.22	-11.11	16.6	18.4	18.4
NoElectronsTracks	$32.6\pm^{0.5}_{0.5}$	$37.6\pm^{1.0}_{1.0}$	33.3±3.4	2.1	-12.91	0.5	0.4	0.9
NoIsoTracks	$31.8\pm^{0.5}_{0.5}$	$36.9\pm^{1.0}_{1.0}$	32.1±3.4	0.93	-14.95	0.8	0.7	1.2
NoIsoPhotons	$31.1\pm^{0.5}_{0.5}$	$36.4\pm^{1.0}_{1.0}$	30.3±3.3	-2.64	-20.13	0.7	0.5	1.8
$\Delta\Phi_{H_T^{miss},j1} > 0.5$	$30.5\pm^{0.5}_{0.5}$	$35.6\pm^{1.0}_{1.0}$	29.5±3.3	-3.39	-20.68	0.6	0.8	0.8
$\Delta\Phi_{H_T^{miss},j2} > 0.5$	$27.9\pm^{0.5}_{0.5}$	$32.2\pm^{1.0}_{1.0}$	26.5±3.2	-5.28	-21.51	2.6	3.4	3.0
$\Delta\Phi_{H_T^{miss},j3} > 0.3$	$26.0\pm^{0.4}_{0.4}$	$30.0\pm^{1.0}_{0.9}$	24.8±3.2	-4.84	-20.97	1.9	2.2	1.7
$\Delta\Phi_{H_T^{miss},j4} > 0.3$	$24.5\pm^{0.4}_{0.4}$	$28.1\pm^{0.9}_{0.9}$	23.1±3.1	-6.06	-21.65	1.5	1.9	1.7

Table 10. Signal yield in the aggregated signal regions for the T1tttt-1900-200 simplified model.

Agg SR	MA5 Pythia8 yield	MA5 Madgraph5+Pythia8 yield	CMS yield	MA5 Pythia8 diff [%]	MA5 Madgraph5+Pythia8 diff [%]
SR1 $N_{jet} \geq 2$ $N_{bjet} = 0$ $H_T > 600$ $H_T^{miss} > 600$	1.38±0.18	2.72±0.5	1.43±0.02	3.5	-90.21
SR2 $N_{jet} \geq 4$ $N_{bjet} = 0$ $H_T > 1700$ $H_T^{miss} > 850$	0.42±0.1	1.27±0.34	0.68±0.02	38.24	-86.76
SR3 $N_{jet} \geq 6$ $N_{bjet} = 0$ $H_T > 600$ $H_T^{miss} > 600$	1.27±0.17	2.63±0.49	1.3±0.02	2.31	-102.31
SR4 $N_{jet} \geq 8$ $N_{bjet} = 0-1$ $H_T > 600$ $H_T^{miss} > 600$	4.72±0.32	7.43±0.82	5.12±0.06	7.81	-45.12
SR5 $N_{jet} \geq 10$ $N_{bjet} = 0-1$ $H_T > 1700$ $H_T^{miss} > 850$	0.71±0.13	2.08±0.43	0.98±0.02	27.55	-112.24
SR6 $N_{jet} \geq 4$ $N_{bjet} \geq 2$ $H_T > 300$ $H_T^{miss} > 300$	41.89±0.97	46.85±2.06	39.89±0.26	-5.01	-17.45
SR7 $N_{jet} \geq 2$ $N_{bjet} \geq 2$ $H_T > 600$ $H_T^{miss} > 600$	22.08±0.7	29.63±1.64	27.13±0.21	18.61	-9.21
SR8 $N_{jet} \geq 6$ $N_{bjet} \geq 2$ $H_T > 350$ $H_T^{miss} > 350$	38.28±0.92	43.68±1.99	37.52±0.25	-2.03	-16.42
SR9 $N_{jet} \geq 4$ $N_{bjet} \geq 2$ $H_T > 600$ $H_T^{miss} > 600$	22.06±0.7	29.63±1.64	27.13±0.21	18.69	-9.21
SR10 $N_{jet} \geq 8$ $N_{bjet} \geq 3$ $H_T > 300$ $H_T^{miss} > 300$	20.79±0.68	24.01±1.48	19.32±0.2	-7.61	-24.28
SR11 $N_{jet} \geq 6$ $N_{bjet} \geq 1$ $H_T > 600$ $H_T^{miss} > 600$	26.91±0.77	36.52±1.82	32.65±0.23	17.58	-11.85
SR12 $N_{jet} \geq 10$ $N_{bjet} \geq 3$ $H_T > 850$ $H_T^{miss} > 850$	2.25±0.22	5.07±0.68	3.69±0.09	39.02	-37.4

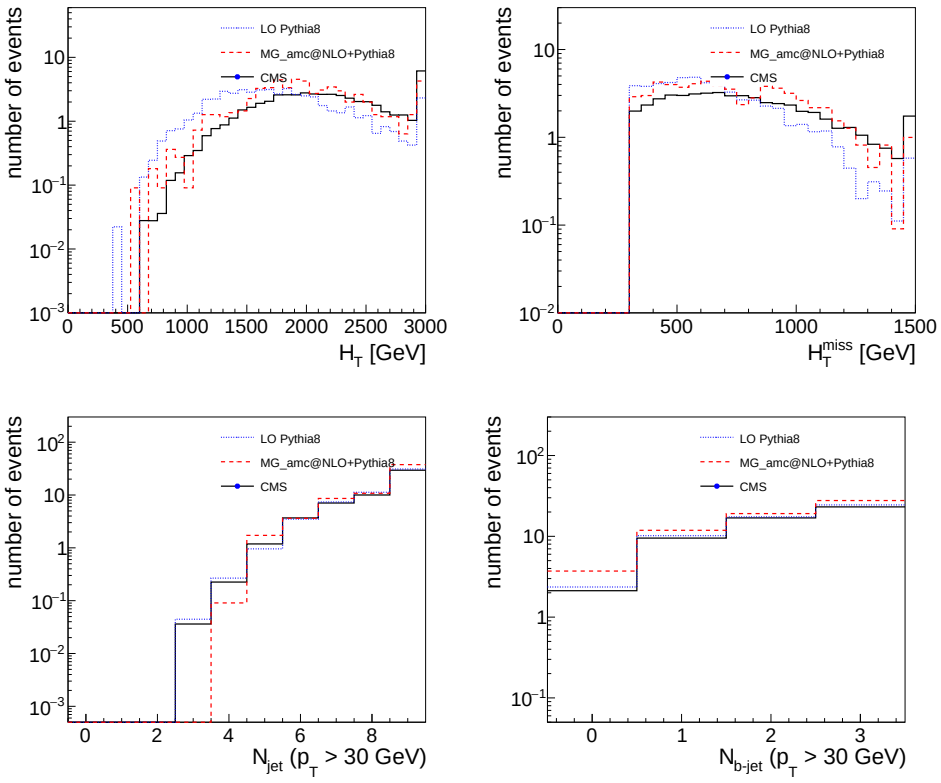

Fig. 6. Kinematic distributions for the T1tttt-1900-200 simplified model for the madanalysis5 implementation and those provided by CMS

Table 11. Pre-selection cutflow for the T1tttt-1300-1000 simplified model.

Cut	MA5 Pythia8	MA5 Madgraph5 +Pythia8	CMS	MA5 Pythia8 diff [%]	MA5 Madgraph5 +Pythia8 diff [%]	MA5 Pythia8 drop [%]	MA5 Madgraph5 +Pythia8 drop [%]	CMS drop [%]
$N_{jet} \geq 2$	$99.9\pm^{0.0}_{0.0}$	$100.0\pm^{0.0}_{0.0}$	100.0±0.0	0.1	0.0	0.1	0.0	0.0
$H_T > 300$	$87.6\pm^{0.3}_{0.3}$	$87.7\pm^{0.3}_{0.3}$	90.1±0.4	2.77	2.66	12.3	12.3	9.9
$H_T^{miss} > 300$	$25.0\pm^{0.4}_{0.4}$	$14.6\pm^{0.3}_{0.3}$	13.8±0.4	-81.16	-5.8	62.6	73.1	76.3
$H_T > H_T^{miss}$	$25.0\pm^{0.4}_{0.4}$	$14.5\pm^{0.3}_{0.3}$	13.8±0.4	-81.16	-5.07	0.0	0.1	0.0
NoIsoMuons	$16.8\pm^{0.4}_{0.4}$	$9.2\pm^{0.3}_{0.3}$	8.8±0.3	-90.91	-4.55	8.2	5.3	5.0
NoMuonsTracks	$16.3\pm^{0.4}_{0.4}$	$9.0\pm^{0.3}_{0.3}$	8.5±0.3	-91.76	-5.88	0.5	0.2	0.3
NoIsoElectrons	$11.2\pm^{0.3}_{0.3}$	$6.5\pm^{0.2}_{0.2}$	5.8±0.3	-93.1	-12.07	5.1	2.5	2.7
NoElectronsTracks	$10.8\pm^{0.3}_{0.3}$	$6.3\pm^{0.2}_{0.2}$	5.4±0.3	-100.0	-16.67	0.4	0.2	0.4
NoIsoTracks	$10.0\pm^{0.3}_{0.3}$	$5.8\pm^{0.2}_{0.2}$	5.0±0.3	-100.0	-16.0	0.8	0.5	0.4
NoIsoPhotons	$10.0\pm^{0.3}_{0.3}$	$5.8\pm^{0.2}_{0.2}$	4.9±0.3	-104.08	-18.37	0.0	0.0	0.1
$\Delta\Phi_{H_T^{miss},j1} > 0.5$	$10.0\pm^{0.3}_{0.3}$	$5.7\pm^{0.2}_{0.2}$	4.9±0.3	-104.08	-16.33	0.0	0.1	0.0
$\Delta\Phi_{H_T^{miss},j2} > 0.5$	$9.1\pm^{0.3}_{0.3}$	$4.8\pm^{0.2}_{0.2}$	4.1±0.2	-121.95	-17.07	0.9	0.9	0.8
$\Delta\Phi_{H_T^{miss},j3} > 0.3$	$8.4\pm^{0.3}_{0.3}$	$4.2\pm^{0.2}_{0.2}$	3.5±0.2	-140.0	-20.0	0.7	0.6	0.6
$\Delta\Phi_{H_T^{miss},j4} > 0.3$	$7.8\pm^{0.3}_{0.3}$	$3.8\pm^{0.2}_{0.2}$	3.1±0.2	-151.61	-22.58	0.6	0.4	0.4

Table 12. Signal yield in the aggregated signal regions for the T1tttt-1300-1000 simplified model.

Agg SR	MA5 Pythia8 yield	MA5 Madgraph5+Pythia8 yield	CMS yield	MA5 Pythia8 diff [%]	MA5 Madgraph5+Pythia8 diff [%]
SR1 $N_{jet} \geq 2$ $N_{bjet} = 0$ $H_T > 600$ $H_T^{miss} > 600$	6.79±2.15	5.47±1.82	2.86±0.17	-137.41	-91.26
SR2 $N_{jet} \geq 4$ $N_{bjet} = 0$ $H_T > 1700$ $H_T^{miss} > 850$	0.68±0.68	0.0±0.0	0.43±0.07	-58.14	100.0
SR3 $N_{jet} \geq 6$ $N_{bjet} = 0$ $H_T > 600$ $H_T^{miss} > 600$	6.11±2.04	5.47±1.82	2.73±0.17	-123.81	-100.37
SR4 $N_{jet} \geq 8$ $N_{bjet} = 0-1$ $H_T > 600$ $H_T^{miss} > 600$	14.95±3.19	14.58±2.98	8.58±0.36	-74.24	-69.93
SR5 $N_{jet} \geq 10$ $N_{bjet} = 0-1$ $H_T > 1700$ $H_T^{miss} > 850$	2.04±1.18	0.61±0.61	0.77±0.09	-164.94	20.78
SR6 $N_{jet} \geq 4$ $N_{bjet} \geq 2$ $H_T > 300$ $H_T^{miss} > 300$	284.66±13.91	137.3±9.13	102.74±1.45	-177.07	-33.64
SR7 $N_{jet} \geq 2$ $N_{bjet} \geq 2$ $H_T > 600$ $H_T^{miss} > 600$	41.44±5.31	25.52±3.94	18.52±0.61	-123.76	-37.8
SR8 $N_{jet} \geq 6$ $N_{bjet} \geq 2$ $H_T > 350$ $H_T^{miss} > 350$	205.85±11.83	101.45±7.85	74.45±1.23	-176.49	-36.27
SR9 $N_{jet} \geq 4$ $N_{bjet} \geq 2$ $H_T > 600$ $H_T^{miss} > 600$	41.44±5.31	25.52±3.94	18.52±0.61	-123.76	-37.8
SR10 $N_{jet} \geq 8$ $N_{bjet} \geq 3$ $H_T > 300$ $H_T^{miss} > 300$	93.75±7.98	34.02±4.55	36.26±0.89	-158.55	6.18
SR11 $N_{jet} \geq 6$ $N_{bjet} \geq 1$ $H_T > 600$ $H_T^{miss} > 600$	57.75±6.26	40.7±4.97	27.2±0.73	-112.32	-49.63
SR12 $N_{jet} \geq 10$ $N_{bjet} \geq 3$ $H_T > 850$ $H_T^{miss} > 850$	1.36±0.96	0.0±0.0	1.26±0.17	-7.94	100.0

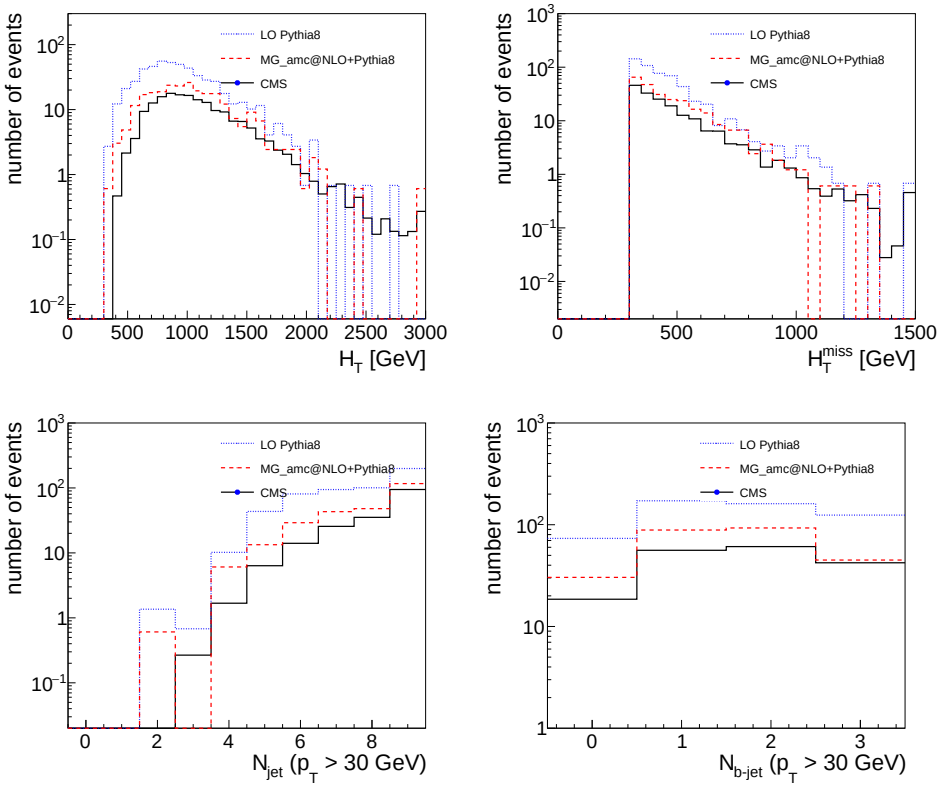

Fig. 7. Kinematic distributions for the T1tttt-1300-1000 simplified model for the madanalysis5 implementation and those provided by CMS

Table 13. Pre-selection cutflow for the T5qqqqVV-1800-100 simplified model.

Cut	MA5 Pythia8	MA5 Madgraph5 +Pythia8	CMS	MA5 Pythia8 diff [%]	MA5 Madgraph5 +Pythia8 diff [%]	MA5 Pythia8 drop [%]	MA5 Madgraph5 +Pythia8 drop [%]	CMS drop [%]
$N_{jet} \geq 2$	$100.0\pm^{0.0}_{0.0}$	$100.0\pm^{0.0}_{0.3}$	100.0±0.5	0.0	0.0	0.0	0.0	0.0
$H_T > 300$	$99.9\pm^{0.0}_{0.0}$	$100.0\pm^{0.0}_{0.3}$	100.0±0.5	0.1	0.0	0.1	0.0	0.0
$H_T^{miss} > 300$	$79.3\pm^{0.4}_{0.4}$	$81.1\pm^{1.6}_{1.7}$	83.0±2.1	4.46	2.29	20.6	18.9	17.0
$H_T > H_T^{miss}$	$79.3\pm^{0.4}_{0.4}$	$81.1\pm^{1.6}_{1.7}$	83.0±2.1	4.46	2.29	0.0	0.0	0.0
NoIsoMuons	$66.6\pm^{0.5}_{0.5}$	$67.5\pm^{1.9}_{1.9}$	68.6±2.5	2.92	1.6	12.7	13.6	14.4
NoMuonsTracks	$66.4\pm^{0.5}_{0.5}$	$67.4\pm^{1.9}_{1.9}$	68.3±2.5	2.78	1.32	0.2	0.1	0.3
NoIsoElectrons	$57.0\pm^{0.5}_{0.5}$	$55.9\pm^{2.0}_{2.0}$	56.1±2.7	-1.6	0.36	9.4	11.5	12.2
NoElectronsTracks	$56.7\pm^{0.5}_{0.5}$	$55.5\pm^{2.0}_{2.0}$	55.6±2.7	-1.98	0.18	0.3	0.4	0.5
NoIsoTracks	$55.7\pm^{0.5}_{0.5}$	$54.4\pm^{2.0}_{2.0}$	53.9±2.7	-3.34	-0.93	1.0	1.1	1.7
NoIsoPhotons	$54.5\pm^{0.5}_{0.5}$	$53.2\pm^{2.0}_{2.0}$	50.6±2.7	-7.71	-5.14	1.2	1.2	3.3
$\Delta\Phi_{H_T^{miss},j1} > 0.5$	$53.8\pm^{0.5}_{0.5}$	$52.7\pm^{2.0}_{2.0}$	49.1±2.7	-9.57	-7.33	0.7	0.5	1.5
$\Delta\Phi_{H_T^{miss},j2} > 0.5$	$49.5\pm^{0.5}_{0.5}$	$48.6\pm^{2.0}_{2.0}$	44.6±2.7	-10.99	-8.97	4.3	4.1	4.5
$\Delta\Phi_{H_T^{miss},j3} > 0.3$	$46.0\pm^{0.5}_{0.5}$	$44.5\pm^{2.0}_{2.0}$	41.6±2.6	-10.58	-6.97	3.5	4.1	3.0
$\Delta\Phi_{H_T^{miss},j4} > 0.3$	$42.5\pm^{0.5}_{0.5}$	$41.8\pm^{2.0}_{2.0}$	38.7±2.6	-9.82	-8.01	3.5	2.7	2.9

Table 14. Signal yield in the aggregated signal regions for the T5qqqqVV-1800-100 simplified model.

Agg SR	MA5 Pythia8 yield	MA5 Madgraph5+Pythia8 yield	CMS yield	MA5 Pythia8 diff [%]	MA5 Madgraph5+Pythia8 diff [%]
SR1 $N_{jet} \geq 2$ $N_{bjet} = 0$ $H_T > 600$ $H_T^{miss} > 600$	62.39±1.54	61.04±5.96	51.62±0.5	-20.86	-18.25
SR2 $N_{jet} \geq 4$ $N_{bjet} = 0$ $H_T > 1700$ $H_T^{miss} > 850$	15.48±0.77	19.18±3.34	19.93±0.31	22.33	3.76
SR3 $N_{jet} \geq 6$ $N_{bjet} = 0$ $H_T > 600$ $H_T^{miss} > 600$	50.87±1.39	56.97±5.75	45.81±0.47	-11.05	-24.36
SR4 $N_{jet} \geq 8$ $N_{bjet} = 0-1$ $H_T > 600$ $H_T^{miss} > 600$	33.29±1.13	44.18±5.07	38.69±0.38	13.96	-14.19
SR5 $N_{jet} \geq 10$ $N_{bjet} = 0-1$ $H_T > 1700$ $H_T^{miss} > 850$	2.82±0.33	3.49±1.42	4.77±0.12	40.88	26.83
SR6 $N_{jet} \geq 4$ $N_{bjet} \geq 2$ $H_T > 300$ $H_T^{miss} > 300$	12.13±0.68	17.44±3.18	15.94±0.14	23.9	-9.41
SR7 $N_{jet} \geq 2$ $N_{bjet} \geq 2$ $H_T > 600$ $H_T^{miss} > 600$	6.79±0.51	9.88±2.4	9.87±0.11	31.21	-0.1
SR8 $N_{jet} \geq 6$ $N_{bjet} \geq 2$ $H_T > 350$ $H_T^{miss} > 350$	10.41±0.63	15.7±3.02	14.43±0.14	27.86	-8.8
SR9 $N_{jet} \geq 4$ $N_{bjet} \geq 2$ $H_T > 600$ $H_T^{miss} > 600$	6.75±0.51	9.88±2.4	9.86±0.11	31.54	-0.2
SR10 $N_{jet} \geq 8$ $N_{bjet} \geq 3$ $H_T > 300$ $H_T^{miss} > 300$	1.14±0.21	2.91±1.3	2.09±0.05	45.45	-39.23
SR11 $N_{jet} \geq 6$ $N_{bjet} \geq 1$ $H_T > 600$ $H_T^{miss} > 600$	23.8±0.95	27.9±4.03	34.51±0.27	31.03	19.15
SR12 $N_{jet} \geq 10$ $N_{bjet} \geq 3$ $H_T > 850$ $H_T^{miss} > 850$	0.08±0.05	1.16±0.82	0.27±0.02	70.37	-329.63

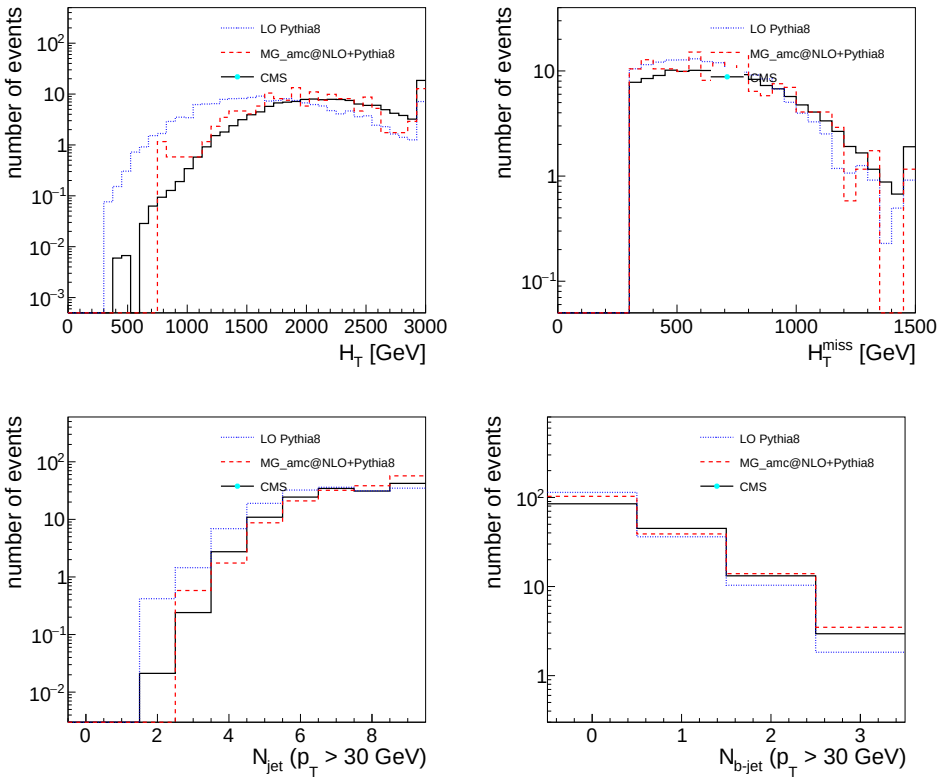

Fig. 8. Kinematic distributions for the T5qqqqVV-1800-100 simplified model for the madanalysis5 implementation and those provided by CMS

Table 15. Pre-selection cutflow for the T5qqqqVV-1400-1100 simplified model.

Cut	MA5 Pythia8	MA5 Madgraph5 +Pythia8	CMS	MA5 Pythia8 diff [%]	MA5 Madgraph5 +Pythia8 diff [%]	MA5 Pythia8 drop [%]	MA5 Madgraph5 +Pythia8 drop [%]	CMS drop [%]
$N_{jet} \geq 2$	$99.6\pm^{0.1}_{0.1}$	$100.0\pm^{0.0}_{0.1}$	100.0±0.1	0.4	0.0	0.4	0.0	0.0
$H_T > 300$	$90.5\pm^{0.3}_{0.3}$	$93.4\pm^{0.5}_{0.5}$	94.6±0.4	4.33	1.27	9.1	6.6	5.4
$H_T^{miss} > 300$	$34.3\pm^{0.5}_{0.5}$	$25.7\pm^{0.9}_{0.8}$	22.2±0.7	-54.5	-15.77	56.2	67.7	72.4
$H_T > H_T^{miss}$	$34.2\pm^{0.5}_{0.5}$	$25.2\pm^{0.8}_{0.8}$	22.1±0.7	-54.75	-14.03	0.1	0.5	0.1
NoIsoMuons	$28.9\pm^{0.5}_{0.5}$	$21.1\pm^{0.8}_{0.8}$	18.5±0.6	-56.22	-14.05	5.3	4.1	3.6
NoMuonsTracks	$28.7\pm^{0.5}_{0.5}$	$20.7\pm^{0.8}_{0.8}$	18.3±0.6	-56.83	-13.11	0.2	0.4	0.2
NoIsoElectrons	$24.4\pm^{0.4}_{0.4}$	$17.6\pm^{0.8}_{0.7}$	15.5±0.6	-57.42	-13.55	4.3	3.1	2.8
NoElectronsTracks	$24.2\pm^{0.4}_{0.4}$	$17.5\pm^{0.7}_{0.7}$	15.1±0.6	-60.26	-15.89	0.2	0.1	0.4
NoIsoTracks	$23.4\pm^{0.4}_{0.4}$	$16.9\pm^{0.7}_{0.7}$	14.4±0.6	-62.5	-17.36	0.8	0.6	0.7
NoIsoPhotons	$23.1\pm^{0.4}_{0.4}$	$16.8\pm^{0.7}_{0.7}$	14.0±0.6	-65.0	-20.0	0.3	0.1	0.4
$\Delta\Phi_{H_T^{miss},j1} > 0.5$	$23.0\pm^{0.4}_{0.4}$	$16.6\pm^{0.7}_{0.7}$	14.0±0.6	-64.29	-18.57	0.1	0.2	0.0
$\Delta\Phi_{H_T^{miss},j2} > 0.5$	$21.5\pm^{0.4}_{0.4}$	$15.2\pm^{0.7}_{0.7}$	12.8±0.6	-67.97	-18.75	1.5	1.4	1.2
$\Delta\Phi_{H_T^{miss},j3} > 0.3$	$20.2\pm^{0.4}_{0.4}$	$14.6\pm^{0.7}_{0.7}$	12.0±0.5	-68.33	-21.67	1.3	0.6	0.8
$\Delta\Phi_{H_T^{miss},j4} > 0.3$	$18.9\pm^{0.4}_{0.4}$	$13.6\pm^{0.7}_{0.7}$	11.2±0.5	-68.75	-21.43	1.3	1.0	0.8

Table 16. Signal yield in the aggregated signal regions for the T5qqqqVV-1400-1100 simplified model.

Agg SR	MA5 Pythia8 yield	MA5 Madgraph5+Pythia8 yield	CMS yield	MA5 Pythia8 diff [%]	MA5 Madgraph5+Pythia8 diff [%]
SR1 $N_{jet} \geq 2$ $N_{bjet} = 0$ $H_T > 600$ $H_T^{miss} > 600$	75.77±5.29	50.4±8.18	29.59±1.1	-156.07	-70.33
SR2 $N_{jet} \geq 4$ $N_{bjet} = 0$ $H_T > 1700$ $H_T^{miss} > 850$	8.87±1.81	2.65±1.88	2.9±0.32	-205.86	8.62
SR3 $N_{jet} \geq 6$ $N_{bjet} = 0$ $H_T > 600$ $H_T^{miss} > 600$	57.29±4.6	46.42±7.85	25.83±1.0	-121.8	-79.71
SR4 $N_{jet} \geq 8$ $N_{bjet} = 0-1$ $H_T > 600$ $H_T^{miss} > 600$	36.96±3.7	35.81±6.89	21.91±0.79	-68.69	-63.44
SR5 $N_{jet} \geq 10$ $N_{bjet} = 0-1$ $H_T > 1700$ $H_T^{miss} > 850$	3.7±1.17	0.0±0.0	1.24±0.17	-198.39	100.0
SR6 $N_{jet} \geq 4$ $N_{bjet} \geq 2$ $H_T > 300$ $H_T^{miss} > 300$	41.03±3.89	26.53±5.93	28.72±0.6	-42.86	7.63
SR7 $N_{jet} \geq 2$ $N_{bjet} \geq 2$ $H_T > 600$ $H_T^{miss} > 600$	7.02±1.61	1.33±1.33	4.34±0.22	-61.75	69.35
SR8 $N_{jet} \geq 6$ $N_{bjet} \geq 2$ $H_T > 350$ $H_T^{miss} > 350$	25.13±3.05	19.89±5.14	18.77±0.48	-33.88	-5.97
SR9 $N_{jet} \geq 4$ $N_{bjet} \geq 2$ $H_T > 600$ $H_T^{miss} > 600$	7.02±1.61	1.33±1.33	4.34±0.22	-61.75	69.35
SR10 $N_{jet} \geq 8$ $N_{bjet} \geq 3$ $H_T > 300$ $H_T^{miss} > 300$	3.33±1.11	6.63±2.97	3.05±0.17	-9.18	-117.38
SR11 $N_{jet} \geq 6$ $N_{bjet} \geq 1$ $H_T > 600$ $H_T^{miss} > 600$	27.35±3.18	14.59±4.4	16.04±0.51	-70.51	9.04
SR12 $N_{jet} \geq 10$ $N_{bjet} \geq 3$ $H_T > 850$ $H_T^{miss} > 850$	0.0±0.0	0.0±0.0	0.1±0.03	100.0	100.0

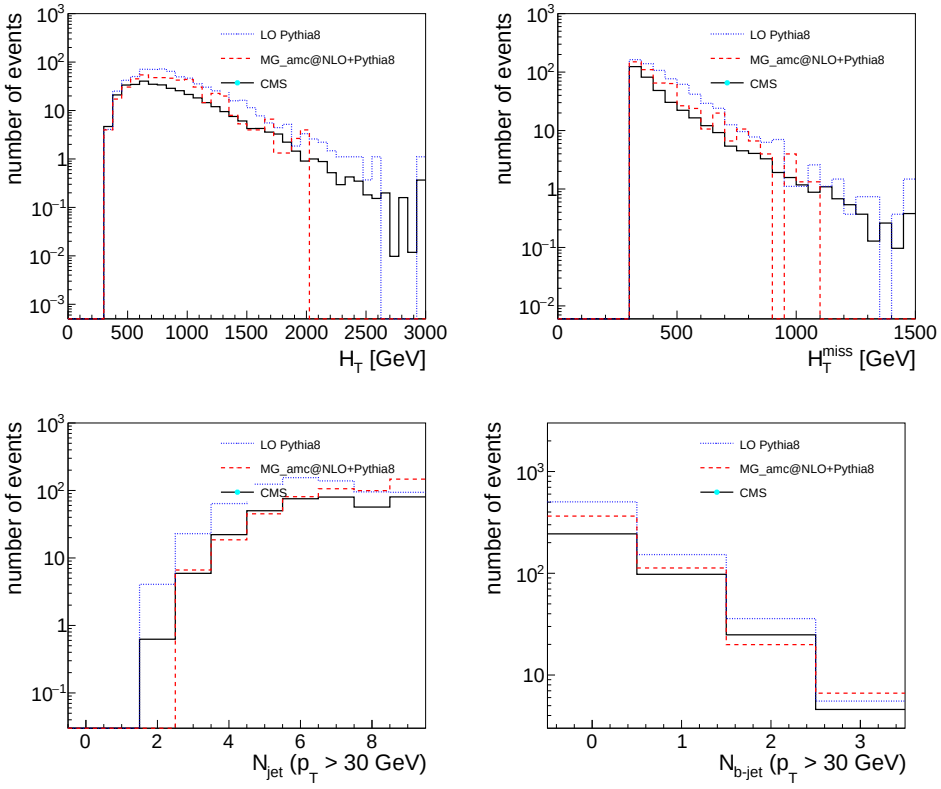

Fig. 9. Kinematic distributions for the T5qqqqVV-1400-1100 simplified model for the madanalysis5 implementation and those provided by CMS

Table 17. Pre-selection cutflow for the T2qq-1400-200 simplified model.

Cut	MA5 Pythia8	MA5 Madgraph5 +Pythia8	CMS	MA5 Pythia8 diff [%]	MA5 Madgraph5 +Pythia8 diff [%]	MA5 Pythia8 drop [%]	MA5 Madgraph5 +Pythia8 drop [%]	CMS drop [%]
$N_{jet} \geq 2$	$99.0\pm^{0.1}_{0.1}$	$99.2\pm^{0.2}_{0.2}$	99.1±0.5	0.1	-0.1	1.0	0.8	0.9
$H_T > 300$	$98.9\pm^{0.1}_{0.1}$	$98.9\pm^{0.2}_{0.3}$	98.9±0.6	0.0	0.0	0.1	0.3	0.2
$H_T^{miss} > 300$	$87.3\pm^{0.3}_{0.3}$	$86.6\pm^{0.7}_{0.8}$	88.1±1.4	0.91	1.7	11.6	12.3	10.8
$H_T > H_T^{miss}$	$86.4\pm^{0.3}_{0.4}$	$85.7\pm^{0.7}_{0.8}$	86.8±1.5	0.46	1.27	0.9	0.9	1.3
NoIsoMuons	$86.4\pm^{0.3}_{0.4}$	$85.6\pm^{0.7}_{0.8}$	86.7±1.5	0.35	1.27	0.0	0.1	0.1
NoMuonsTracks	$86.3\pm^{0.3}_{0.4}$	$85.6\pm^{0.7}_{0.8}$	86.7±1.5	0.46	1.27	0.1	0.0	0.0
NoIsoElectrons	$86.3\pm^{0.3}_{0.4}$	$85.6\pm^{0.7}_{0.8}$	86.4±1.5	0.12	0.93	0.0	0.0	0.3
NoElectronsTracks	$86.2\pm^{0.3}_{0.4}$	$85.6\pm^{0.7}_{0.8}$	86.2±1.5	0.0	0.7	0.1	0.0	0.2
NoIsoTracks	$86.1\pm^{0.3}_{0.4}$	$85.3\pm^{0.7}_{0.8}$	85.6±1.5	-0.58	0.35	0.1	0.3	0.6
NoIsoPhotons	$84.6\pm^{0.4}_{0.4}$	$84.3\pm^{0.8}_{0.8}$	83.6±1.6	-1.2	-0.84	1.5	1.0	2.0
$\Delta\Phi_{H_T^{miss},j1} > 0.5$	$84.5\pm^{0.4}_{0.4}$	$84.3\pm^{0.8}_{0.8}$	83.5±1.6	-1.2	-0.96	0.1	0.0	0.1
$\Delta\Phi_{H_T^{miss},j2} > 0.5$	$80.0\pm^{0.4}_{0.4}$	$80.5\pm^{0.8}_{0.9}$	78.7±1.7	-1.65	-2.29	4.5	3.8	4.8
$\Delta\Phi_{H_T^{miss},j3} > 0.3$	$76.0\pm^{0.4}_{0.4}$	$76.5\pm^{0.9}_{0.9}$	74.4±1.8	-2.15	-2.82	4.0	4.0	4.3
$\Delta\Phi_{H_T^{miss},j4} > 0.3$	$73.3\pm^{0.4}_{0.4}$	$74.3\pm^{0.9}_{1.0}$	71.4±1.9	-2.66	-4.06	2.7	2.2	3.0

Table 18. Signal yield in the aggregated signal regions for the T2qq-1400-200 simplified model.

Agg SR	MA5 Pythia8 yield	MA5 Madgraph5+Pythia8 yield	CMS yield	MA5 Pythia8 diff [%]	MA5 Madgraph5+Pythia8 diff [%]
SR1 $N_{jet} \geq 2$ $N_{bjet} = 0$ $H_T > 600$ $H_T^{miss} > 600$	252.25±3.54	233.98±7.16	285.27±2.44	11.57	17.98
SR2 $N_{jet} \geq 4$ $N_{bjet} = 0$ $H_T > 1700$ $H_T^{miss} > 850$	39.93±1.41	40.97±3.0	35.93±0.81	-11.13	-14.03
SR3 $N_{jet} \geq 6$ $N_{bjet} = 0$ $H_T > 600$ $H_T^{miss} > 600$	25.68±1.13	38.56±2.91	33.64±0.72	23.66	-14.63
SR4 $N_{jet} \geq 8$ $N_{bjet} = 0-1$ $H_T > 600$ $H_T^{miss} > 600$	3.87±0.44	8.76±1.39	7.19±0.28	46.18	-21.84
SR5 $N_{jet} \geq 10$ $N_{bjet} = 0-1$ $H_T > 1700$ $H_T^{miss} > 850$	0.2±0.1	0.22±0.22	0.4±0.06	50.0	45.0
SR6 $N_{jet} \geq 4$ $N_{bjet} \geq 2$ $H_T > 300$ $H_T^{miss} > 300$	2.68±0.36	5.26±1.07	5.17±0.15	48.16	-1.74
SR7 $N_{jet} \geq 2$ $N_{bjet} \geq 2$ $H_T > 600$ $H_T^{miss} > 600$	2.33±0.34	5.04±1.05	4.55±0.12	48.79	-10.77
SR8 $N_{jet} \geq 6$ $N_{bjet} \geq 2$ $H_T > 350$ $H_T^{miss} > 350$	1.14±0.24	2.85±0.79	2.38±0.1	52.1	-19.75
SR9 $N_{jet} \geq 4$ $N_{bjet} \geq 2$ $H_T > 600$ $H_T^{miss} > 600$	2.09±0.32	3.72±0.9	3.72±0.12	43.82	0.0
SR10 $N_{jet} \geq 8$ $N_{bjet} \geq 3$ $H_T > 300$ $H_T^{miss} > 300$	0.05±0.05	0.0±0.0	0.12±0.03	58.33	100.0
SR11 $N_{jet} \geq 6$ $N_{bjet} \geq 1$ $H_T > 600$ $H_T^{miss} > 600$	4.67±0.48	7.45±1.28	10.6±0.24	55.94	29.72
SR12 $N_{jet} \geq 10$ $N_{bjet} \geq 3$ $H_T > 850$ $H_T^{miss} > 850$	0.0±0.0	0.0±0.0	0.02±0.01	100.0	100.0

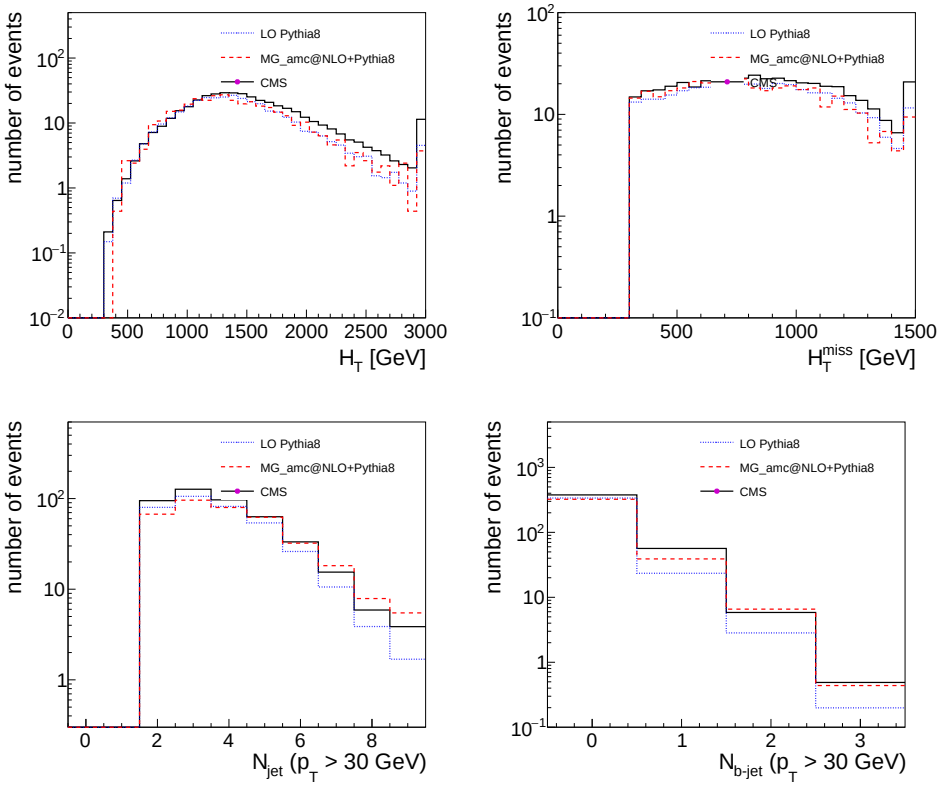

Fig. 10. Kinematic distributions for the T2qq-1400-200 simplified model for the madanalysis5 implementation and those provided by CMS

Table 19. Pre-selection cutflow for the T2qq-1000-800 simplified model.

Cut	MA5 Pythia8	MA5 Madgraph5 +Pythia8	CMS	MA5 Pythia8 diff [%]	MA5 Madgraph5 +Pythia8 diff [%]	MA5 Pythia8 drop [%]	MA5 Madgraph5 +Pythia8 drop [%]	CMS drop [%]
$N_{jet} \geq 2$	$95.6\pm^{0.2}_{0.2}$	$97.9\pm^{0.1}_{0.1}$	97.8±0.2	2.25	-0.1	4.4	2.1	2.2
$H_T > 300$	$76.0\pm^{0.4}_{0.4}$	$80.5\pm^{0.4}_{0.4}$	83.0±0.4	8.43	3.01	19.6	17.4	14.8
$H_T^{miss} > 300$	$28.7\pm^{0.5}_{0.5}$	$28.5\pm^{0.4}_{0.4}$	31.3±0.5	8.31	8.95	47.3	52.0	51.7
$H_T > H_T^{miss}$	$28.0\pm^{0.5}_{0.5}$	$27.7\pm^{0.4}_{0.4}$	30.2±0.5	7.28	8.28	0.7	0.8	1.1
NoIsoMuons	$28.0\pm^{0.5}_{0.5}$	$27.7\pm^{0.4}_{0.4}$	30.1±0.5	6.98	7.97	0.0	0.0	0.1
NoMuonsTracks	$28.0\pm^{0.5}_{0.5}$	$27.7\pm^{0.4}_{0.4}$	30.1±0.5	6.98	7.97	0.0	0.0	0.0
NoIsoElectrons	$28.0\pm^{0.5}_{0.5}$	$27.6\pm^{0.4}_{0.4}$	30.0±0.5	6.67	8.0	0.0	0.1	0.1
NoElectronsTracks	$28.0\pm^{0.5}_{0.5}$	$27.6\pm^{0.4}_{0.4}$	29.9±0.5	6.35	7.69	0.0	0.0	0.1
NoIsoTracks	$27.8\pm^{0.5}_{0.5}$	$27.5\pm^{0.4}_{0.4}$	29.6±0.5	6.08	7.09	0.2	0.1	0.3
NoIsoPhotons	$27.5\pm^{0.5}_{0.4}$	$27.3\pm^{0.4}_{0.4}$	28.8±0.5	4.51	5.21	0.3	0.2	0.8
$\Delta\Phi_{H_T^{miss},j1} > 0.5$	$27.5\pm^{0.5}_{0.4}$	$27.3\pm^{0.4}_{0.4}$	28.8±0.5	4.51	5.21	0.0	0.0	0.0
$\Delta\Phi_{H_T^{miss},j2} > 0.5$	$26.1\pm^{0.4}_{0.4}$	$25.9\pm^{0.4}_{0.4}$	27.1±0.5	3.69	4.43	1.4	1.4	1.7
$\Delta\Phi_{H_T^{miss},j3} > 0.3$	$25.2\pm^{0.4}_{0.4}$	$25.0\pm^{0.4}_{0.4}$	26.0±0.5	3.08	3.85	0.9	0.9	1.1
$\Delta\Phi_{H_T^{miss},j4} > 0.3$	$24.6\pm^{0.4}_{0.4}$	$24.2\pm^{0.4}_{0.4}$	25.2±0.5	2.38	3.97	0.6	0.8	0.8

Table 20. Signal yield in the aggregated signal regions for the T2qq-1000-800 simplified model.

Agg SR	MA5 Pythia8 yield	MA5 Madgraph5+Pythia8 yield	CMS yield	MA5 Pythia8 diff [%]	MA5 Madgraph5+Pythia8 diff [%]
SR1 $N_{jet} \geq 2$ $N_{bjet} = 0$ $H_T > 600$ $H_T^{miss} > 600$	166.19±10.91	172.66±10.51	188.65±4.54	11.91	8.48
SR2 $N_{jet} \geq 4$ $N_{bjet} = 0$ $H_T > 1700$ $H_T^{miss} > 850$	5.01±1.9	7.67±2.22	10.1±0.96	50.4	24.06
SR3 $N_{jet} \geq 6$ $N_{bjet} = 0$ $H_T > 600$ $H_T^{miss} > 600$	32.24±4.81	45.4±5.39	48.21±1.99	33.13	5.83
SR4 $N_{jet} \geq 8$ $N_{bjet} = 0-1$ $H_T > 600$ $H_T^{miss} > 600$	5.73±2.03	10.23±2.56	11.76±0.77	51.28	13.01
SR5 $N_{jet} \geq 10$ $N_{bjet} = 0-1$ $H_T > 1700$ $H_T^{miss} > 850$	0.0±0.0	0.64±0.64	0.34±0.11	100.0	-88.24
SR6 $N_{jet} \geq 4$ $N_{bjet} \geq 2$ $H_T > 300$ $H_T^{miss} > 300$	12.18±2.95	26.86±4.14	23.23±0.61	47.57	-15.63
SR7 $N_{jet} \geq 2$ $N_{bjet} \geq 2$ $H_T > 600$ $H_T^{miss} > 600$	2.15±1.24	7.67±2.22	4.57±0.26	52.95	-67.83
SR8 $N_{jet} \geq 6$ $N_{bjet} \geq 2$ $H_T > 350$ $H_T^{miss} > 350$	3.58±1.6	14.71±3.07	8.68±0.39	58.76	-69.47
SR9 $N_{jet} \geq 4$ $N_{bjet} \geq 2$ $H_T > 600$ $H_T^{miss} > 600$	2.15±1.24	7.03±2.12	4.23±0.25	49.17	-66.19
SR10 $N_{jet} \geq 8$ $N_{bjet} \geq 3$ $H_T > 300$ $H_T^{miss} > 300$	0.0±0.0	0.64±0.64	0.36±0.07	100.0	-77.78
SR11 $N_{jet} \geq 6$ $N_{bjet} \geq 1$ $H_T > 600$ $H_T^{miss} > 600$	2.87±1.43	17.27±3.32	14.65±0.62	80.41	-17.88
SR12 $N_{jet} \geq 10$ $N_{bjet} \geq 3$ $H_T > 850$ $H_T^{miss} > 850$	0.0±0.0	0.0±0.0	0.0±0.0	nan	nan

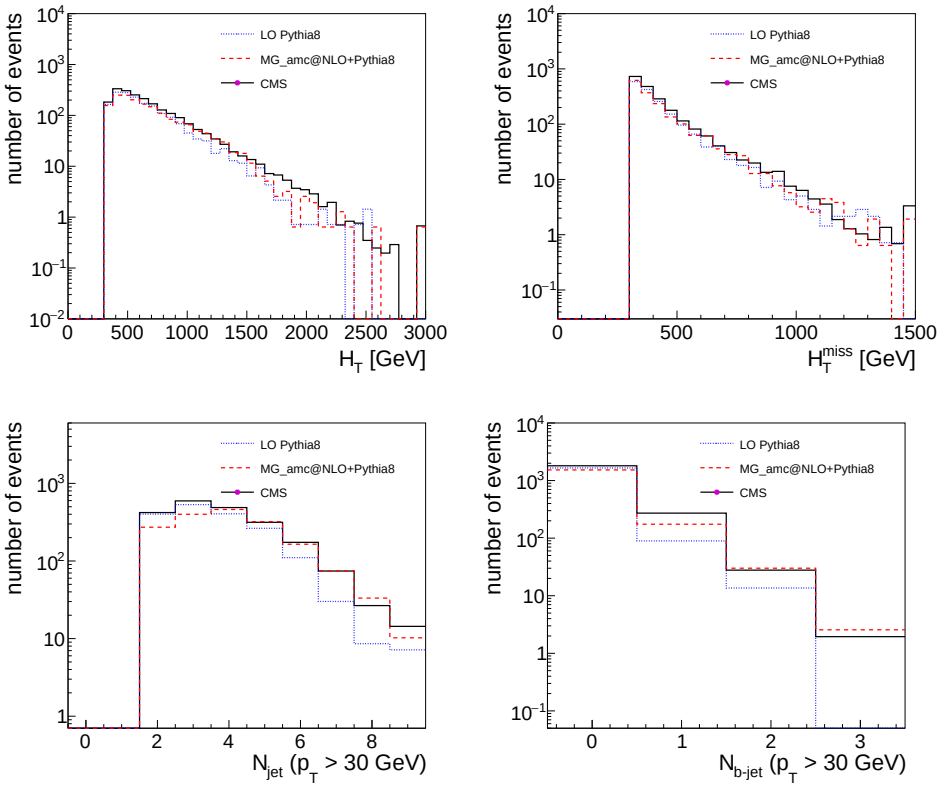

Fig. 11. Kinematic distributions for the T2qq-1000-800 simplified model for the madanalysis5 implementation and those provided by CMS

Table 21. Pre-selection cutflow for the T2bb-1000-100 simplified model.

Cut	MA5 Pythia8	MA5 Madgraph5 +Pythia8	CMS	MA5 Pythia8 diff [%]	MA5 Madgraph5 +Pythia8 diff [%]	MA5 Pythia8 drop [%]	MA5 Madgraph5 +Pythia8 drop [%]	CMS drop [%]
$N_{jet} \geq 2$	$98.8\pm^{0.1}_{0.1}$	$99.2\pm^{0.2}_{0.2}$	98.8±0.5	0.0	-0.4	1.2	0.8	1.2
$H_T > 300$	$98.2\pm^{0.1}_{0.1}$	$98.8\pm^{0.2}_{0.3}$	98.3±0.5	0.1	-0.51	0.6	0.4	0.5
$H_T^{miss} > 300$	$78.4\pm^{0.4}_{0.4}$	$78.2\pm^{0.9}_{0.9}$	79.6±1.4	1.51	1.76	19.8	20.6	18.7
$H_T > H_T^{miss}$	$77.3\pm^{0.4}_{0.4}$	$77.3\pm^{0.9}_{0.9}$	78.2±1.4	1.15	1.15	1.1	0.9	1.4
NoIsoMuons	$77.2\pm^{0.4}_{0.4}$	$77.2\pm^{0.9}_{0.9}$	77.9±1.4	0.9	0.9	0.1	0.1	0.3
NoMuonsTracks	$77.2\pm^{0.4}_{0.4}$	$77.2\pm^{0.9}_{0.9}$	77.8±1.4	0.77	0.77	0.0	0.0	0.1
NoIsoElectrons	$77.1\pm^{0.4}_{0.4}$	$77.0\pm^{0.9}_{0.9}$	77.5±1.5	0.52	0.65	0.1	0.2	0.3
NoElectronsTracks	$77.0\pm^{0.4}_{0.4}$	$76.7\pm^{0.9}_{0.9}$	77.2±1.5	0.26	0.65	0.1	0.3	0.3
NoIsoTracks	$76.9\pm^{0.4}_{0.4}$	$76.4\pm^{0.9}_{0.9}$	76.8±1.5	-0.13	0.52	0.1	0.3	0.4
NoIsoPhotons	$76.4\pm^{0.4}_{0.4}$	$75.8\pm^{0.9}_{0.9}$	75.2±1.5	-1.6	-0.8	0.5	0.6	1.6
$\Delta\Phi_{H_T^{miss},j1} > 0.5$	$76.3\pm^{0.4}_{0.4}$	$75.7\pm^{0.9}_{0.9}$	75.1±1.5	-1.6	-0.8	0.1	0.1	0.1
$\Delta\Phi_{H_T^{miss},j2} > 0.5$	$72.3\pm^{0.5}_{0.5}$	$72.0\pm^{1.0}_{1.0}$	70.6±1.6	-2.41	-1.98	4.0	3.7	4.5
$\Delta\Phi_{H_T^{miss},j3} > 0.3$	$68.9\pm^{0.5}_{0.5}$	$68.2\pm^{1.0}_{1.0}$	67.0±1.6	-2.84	-1.79	3.4	3.8	3.6
$\Delta\Phi_{H_T^{miss},j4} > 0.3$	$66.5\pm^{0.5}_{0.5}$	$65.4\pm^{1.0}_{1.0}$	64.5±1.6	-3.1	-1.4	2.4	2.8	2.5

Table 22. Signal yield in the aggregated signal regions for the T2bb-1000-100 simplified model.

Agg SR	MA5 Pythia8 yield	MA5 Madgraph5+Pythia8 yield	CMS yield	MA5 Pythia8 diff [%]	MA5 Madgraph5+Pythia8 diff [%]
SR1 $N_{jet} \geq 2$ $N_{bjet} = 0$ $H_T > 600$ $H_T^{miss} > 600$	58.4±2.28	52.59±4.56	81.08±0.94	27.97	35.14
SR2 $N_{jet} \geq 4$ $N_{bjet} = 0$ $H_T > 1700$ $H_T^{miss} > 850$	3.38±0.55	4.75±1.37	3.24±0.19	-4.32	-46.6
SR3 $N_{jet} \geq 6$ $N_{bjet} = 0$ $H_T > 600$ $H_T^{miss} > 600$	4.44±0.63	7.12±1.68	7.38±0.22	39.84	3.52
SR4 $N_{jet} \geq 8$ $N_{bjet} = 0-1$ $H_T > 600$ $H_T^{miss} > 600$	1.87±0.41	3.56±1.19	3.38±0.16	44.67	-5.33
SR5 $N_{jet} \geq 10$ $N_{bjet} = 0-1$ $H_T > 1700$ $H_T^{miss} > 850$	0.0±0.0	0.0±0.0	0.11±0.03	100.0	100.0
SR6 $N_{jet} \geq 4$ $N_{bjet} \geq 2$ $H_T > 300$ $H_T^{miss} > 300$	116.89±3.22	133.26±7.26	84.14±0.85	-38.92	-58.38
SR7 $N_{jet} \geq 2$ $N_{bjet} \geq 2$ $H_T > 600$ $H_T^{miss} > 600$	109.07±3.11	102.42±6.36	76.83±0.81	-41.96	-33.31
SR8 $N_{jet} \geq 6$ $N_{bjet} \geq 2$ $H_T > 350$ $H_T^{miss} > 350$	28.53±1.59	35.19±3.73	23.03±0.43	-23.88	-52.8
SR9 $N_{jet} \geq 4$ $N_{bjet} \geq 2$ $H_T > 600$ $H_T^{miss} > 600$	60.36±2.32	67.22±5.16	43.57±0.6	-38.54	-54.28
SR10 $N_{jet} \geq 8$ $N_{bjet} \geq 3$ $H_T > 300$ $H_T^{miss} > 300$	1.33±0.34	1.58±0.79	1.01±0.08	-31.68	-56.44
SR11 $N_{jet} \geq 6$ $N_{bjet} \geq 1$ $H_T > 600$ $H_T^{miss} > 600$	27.56±1.57	33.61±3.65	29.97±0.54	8.04	-12.15
SR12 $N_{jet} \geq 10$ $N_{bjet} \geq 3$ $H_T > 850$ $H_T^{miss} > 850$	0.09±0.09	0.0±0.0	0.04±0.02	-125.0	100.0

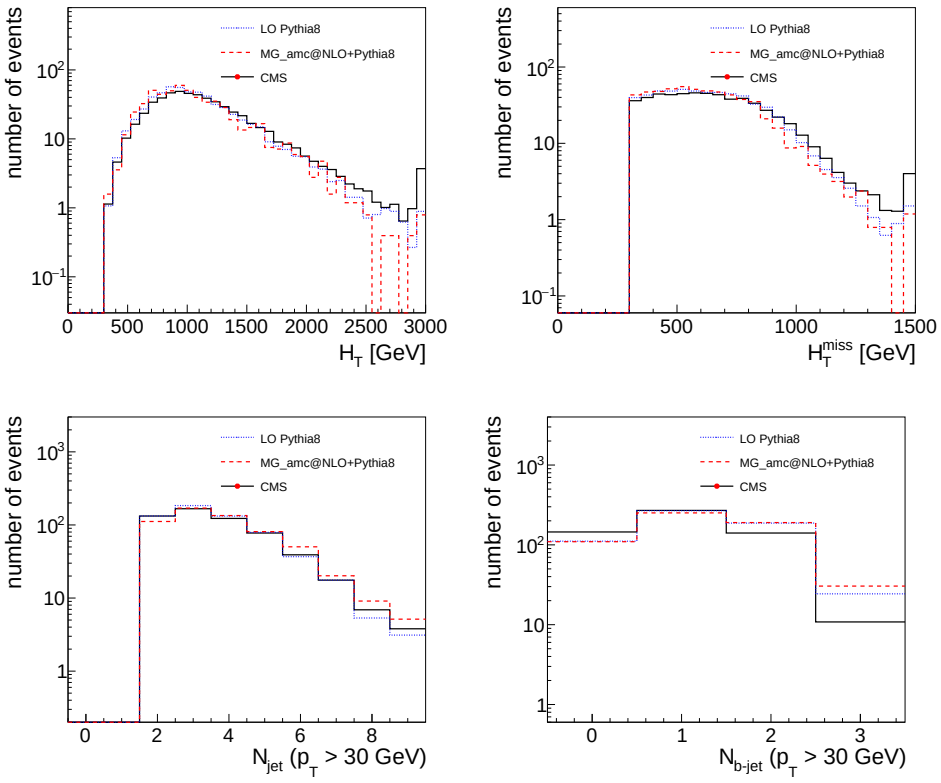

Fig. 12. Kinematic distributions for the T2bb-1000-100 simplified model for the madanalysis5 implementation and those provided by CMS

Table 23. Pre-selection cutflow for the T2bb-600-450 simplified model.

Cut	MA5 Pythia8	MA5 Madgraph5 +Pythia8	CMS	MA5 Pythia8 diff [%]	MA5 Madgraph5 +Pythia8 diff [%]	MA5 Pythia8 drop [%]	MA5 Madgraph5 +Pythia8 drop [%]	CMS drop [%]
$N_{jet} \geq 2$	$95.0\pm^{0.2}_{0.2}$	$95.2\pm^{0.4}_{0.5}$	95.4±0.1	0.42	0.21	5.0	4.8	4.6
$H_T > 300$	$54.1\pm^{0.5}_{0.5}$	$56.5\pm^{1.0}_{1.0}$	58.2±0.3	7.04	2.92	40.9	38.7	37.2
$H_T^{miss} > 300$	$11.0\pm^{0.3}_{0.3}$	$12.4\pm^{0.7}_{0.7}$	13.6±0.2	19.12	8.82	43.1	44.1	44.6
$H_T > H_T^{miss}$	$10.7\pm^{0.3}_{0.3}$	$12.2\pm^{0.7}_{0.7}$	13.2±0.2	18.94	7.58	0.3	0.2	0.4
NoIsoMuons	$10.7\pm^{0.3}_{0.3}$	$12.1\pm^{0.7}_{0.7}$	13.1±0.2	18.32	7.63	0.0	0.1	0.1
NoMuonsTracks	$10.7\pm^{0.3}_{0.3}$	$12.1\pm^{0.7}_{0.7}$	13.1±0.2	18.32	7.63	0.0	0.0	0.0
NoIsoElectrons	$10.7\pm^{0.3}_{0.3}$	$12.1\pm^{0.7}_{0.7}$	13.0±0.2	17.69	6.92	0.0	0.0	0.1
NoElectronsTracks	$10.6\pm^{0.3}_{0.3}$	$12.0\pm^{0.7}_{0.7}$	12.9±0.2	17.83	6.98	0.1	0.1	0.1
NoIsoTracks	$10.6\pm^{0.3}_{0.3}$	$12.0\pm^{0.7}_{0.7}$	12.8±0.2	17.19	6.25	0.0	0.0	0.1
NoIsoPhotons	$10.5\pm^{0.3}_{0.3}$	$11.9\pm^{0.7}_{0.7}$	12.5±0.2	16.0	4.8	0.1	0.1	0.3
$\Delta\Phi_{H_T^{miss},j1} > 0.5$	$10.5\pm^{0.3}_{0.3}$	$11.9\pm^{0.7}_{0.7}$	12.5±0.2	16.0	4.8	0.0	0.0	0.0
$\Delta\Phi_{H_T^{miss},j2} > 0.5$	$9.8\pm^{0.3}_{0.3}$	$10.8\pm^{0.7}_{0.6}$	11.3±0.2	13.27	4.42	0.7	1.1	1.2
$\Delta\Phi_{H_T^{miss},j3} > 0.3$	$9.3\pm^{0.3}_{0.3}$	$10.4\pm^{0.7}_{0.6}$	10.7±0.2	13.08	2.8	0.5	0.4	0.6
$\Delta\Phi_{H_T^{miss},j4} > 0.3$	$9.0\pm^{0.3}_{0.3}$	$10.0\pm^{0.7}_{0.6}$	10.2±0.2	11.76	1.96	0.3	0.4	0.5

Table 24. Signal yield in the aggregated signal regions for the T2bb-600-450 simplified model.

Agg SR	MA5 Pythia8 yield	MA5 Madgraph5+Pythia8 yield	CMS yield	MA5 Pythia8 diff [%]	MA5 Madgraph5+Pythia8 diff [%]
SR1 $N_{jet} \geq 2$ $N_{bjet} = 0$ $H_T > 600$ $H_T^{miss} > 600$	21.34±7.55	0.0±0.0	30.02±0.66	28.91	100.0
SR2 $N_{jet} \geq 4$ $N_{bjet} = 0$ $H_T > 1700$ $H_T^{miss} > 850$	0.0±0.0	0.0±0.0	0.84±0.09	100.0	100.0
SR3 $N_{jet} \geq 6$ $N_{bjet} = 0$ $H_T > 600$ $H_T^{miss} > 600$	5.34±3.77	0.0±0.0	6.0±0.21	11.0	100.0
SR4 $N_{jet} \geq 8$ $N_{bjet} = 0-1$ $H_T > 600$ $H_T^{miss} > 600$	2.67±2.67	11.1±11.1	4.93±0.27	45.84	-125.15
SR5 $N_{jet} \geq 10$ $N_{bjet} = 0-1$ $H_T > 1700$ $H_T^{miss} > 850$	0.0±0.0	0.0±0.0	0.15±0.05	100.0	100.0
SR6 $N_{jet} \geq 4$ $N_{bjet} \geq 2$ $H_T > 300$ $H_T^{miss} > 300$	632.33±41.07	843.84±96.79	682.87±4.09	7.4	-23.57
SR7 $N_{jet} \geq 2$ $N_{bjet} \geq 2$ $H_T > 600$ $H_T^{miss} > 600$	64.03±13.07	99.93±33.31	90.18±1.49	29.0	-10.81
SR8 $N_{jet} \geq 6$ $N_{bjet} \geq 2$ $H_T > 350$ $H_T^{miss} > 350$	117.4±17.7	288.68±56.61	143.37±1.69	18.11	-101.35
SR9 $N_{jet} \geq 4$ $N_{bjet} \geq 2$ $H_T > 600$ $H_T^{miss} > 600$	53.36±11.93	88.82±31.4	74.32±1.31	28.2	-19.51
SR10 $N_{jet} \geq 8$ $N_{bjet} \geq 3$ $H_T > 300$ $H_T^{miss} > 300$	0.0±0.0	22.21±15.7	6.33±0.28	100.0	-250.87
SR11 $N_{jet} \geq 6$ $N_{bjet} \geq 1$ $H_T > 600$ $H_T^{miss} > 600$	32.02±9.24	88.82±31.4	51.75±1.01	38.13	-71.63
SR12 $N_{jet} \geq 10$ $N_{bjet} \geq 3$ $H_T > 850$ $H_T^{miss} > 850$	0.0±0.0	0.0±0.0	0.07±0.03	100.0	100.0

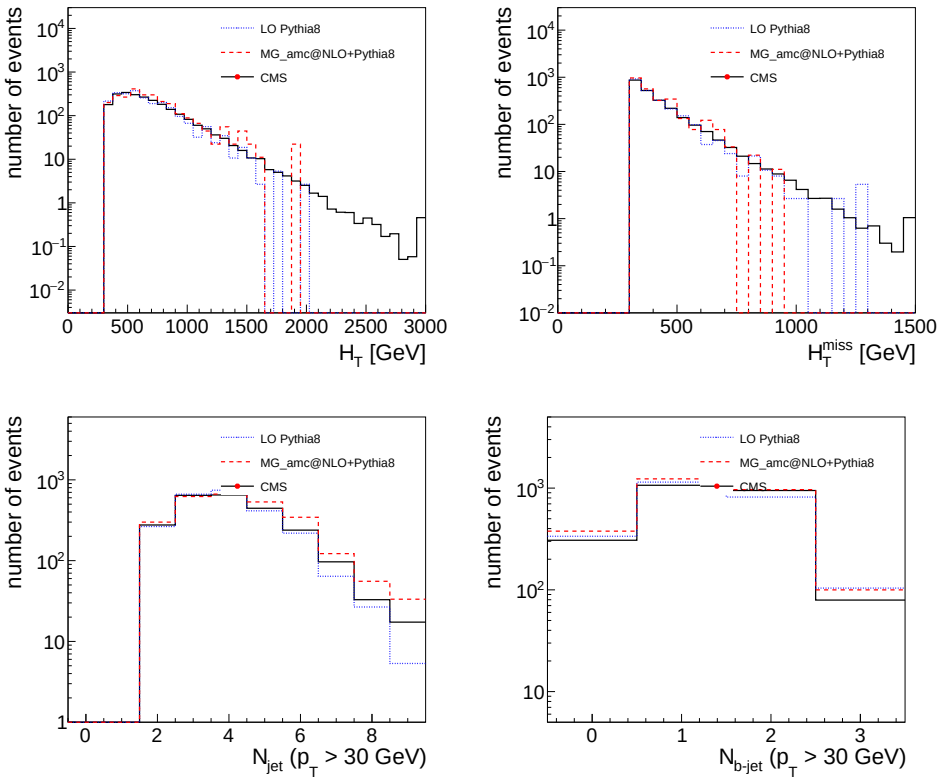

Fig. 13. Kinematic distributions for the T2bb-600-450 simplified model for the madanalysis5 implementation and those provided by CMS

Table 25. Pre-selection cutflow for the T2tt-950-100 simplified model.

Cut	MA5 Pythia8	MA5 Madgraph5 +Pythia8	CMS	MA5 Pythia8 diff [%]	MA5 Madgraph5 +Pythia8 diff [%]	MA5 Pythia8 drop [%]	MA5 Madgraph5 +Pythia8 drop [%]	CMS drop [%]
$N_{jet} \geq 2$	$99.8\pm^{0.0}_{0.1}$	$99.9\pm^{0.1}_{0.1}$	99.9±0.2	0.1	0.0	0.2	0.1	0.1
$H_T > 300$	$98.3\pm^{0.1}_{0.1}$	$97.9\pm^{0.3}_{0.3}$	98.7±0.4	0.41	0.81	1.5	2.0	1.2
$H_T^{miss} > 300$	$72.2\pm^{0.5}_{0.5}$	$68.9\pm^{1.0}_{1.0}$	74.5±1.2	3.09	7.52	26.1	29.0	24.2
$H_T > H_T^{miss}$	$71.3\pm^{0.5}_{0.5}$	$68.3\pm^{1.0}_{1.0}$	73.6±1.3	3.12	7.2	0.9	0.6	0.9
NoIsoMuons	$58.1\pm^{0.5}_{0.5}$	$56.4\pm^{1.1}_{1.1}$	58.7±1.4	1.02	3.92	13.2	11.9	14.9
NoMuonsTracks	$57.7\pm^{0.5}_{0.5}$	$55.8\pm^{1.1}_{1.1}$	58.2±1.4	0.86	4.12	0.4	0.6	0.5
NoIsoElectrons	$47.3\pm^{0.5}_{0.5}$	$45.7\pm^{1.1}_{1.1}$	47.2±1.4	-0.21	3.18	10.4	10.1	11.0
NoElectronsTracks	$46.9\pm^{0.5}_{0.5}$	$45.5\pm^{1.1}_{1.1}$	46.4±1.4	-1.08	1.94	0.4	0.2	0.8
NoIsoTracks	$46.6\pm^{0.5}_{0.5}$	$45.3\pm^{1.1}_{1.1}$	45.5±1.4	-2.42	0.44	0.3	0.2	0.9
NoIsoPhotons	$46.0\pm^{0.5}_{0.5}$	$44.6\pm^{1.1}_{1.1}$	43.8±1.4	-5.02	-1.83	0.6	0.7	1.7
$\Delta\Phi_{H_T^{miss},j1} > 0.5$	$45.8\pm^{0.5}_{0.5}$	$44.5\pm^{1.1}_{1.1}$	43.6±1.4	-5.05	-2.06	0.2	0.1	0.2
$\Delta\Phi_{H_T^{miss},j2} > 0.5$	$43.7\pm^{0.5}_{0.5}$	$42.1\pm^{1.1}_{1.1}$	41.1±1.4	-6.33	-2.43	2.1	2.4	2.5
$\Delta\Phi_{H_T^{miss},j3} > 0.3$	$42.4\pm^{0.5}_{0.5}$	$41.0\pm^{1.1}_{1.0}$	39.8±1.4	-6.53	-3.02	1.3	1.1	1.3
$\Delta\Phi_{H_T^{miss},j4} > 0.3$	$41.0\pm^{0.5}_{0.5}$	$39.5\pm^{1.1}_{1.0}$	38.5±1.4	-6.49	-2.6	1.4	1.5	1.3

Table 26. Signal yield in the aggregated signal regions for the T2tt-950-100 simplified model.

Agg SR	MA5 Pythia8 yield	MA5 Madgraph5+Pythia8 yield	CMS yield	MA5 Pythia8 diff [%]	MA5 Madgraph5+Pythia8 diff [%]
SR1 $N_{jet} \geq 2$ $N_{bjet} = 0$ $H_T > 600$ $H_T^{miss} > 600$	36.37±2.17	32.91±4.32	40.94±0.5	11.16	19.61
SR2 $N_{jet} \geq 4$ $N_{bjet} = 0$ $H_T > 1700$ $H_T^{miss} > 850$	1.16±0.39	0.57±0.57	1.56±0.1	25.64	63.46
SR3 $N_{jet} \geq 6$ $N_{bjet} = 0$ $H_T > 600$ $H_T^{miss} > 600$	11.61±1.22	11.92±2.6	13.38±0.23	13.23	10.91
SR4 $N_{jet} \geq 8$ $N_{bjet} = 0-1$ $H_T > 600$ $H_T^{miss} > 600$	11.74±1.23	10.21±2.41	12.77±0.27	8.07	20.05
SR5 $N_{jet} \geq 10$ $N_{bjet} = 0-1$ $H_T > 1700$ $H_T^{miss} > 850$	0.26±0.18	0.0±0.0	0.28±0.04	7.14	100.0
SR6 $N_{jet} \geq 4$ $N_{bjet} \geq 2$ $H_T > 300$ $H_T^{miss} > 300$	181.99±4.84	197.47±10.59	181.57±1.13	-0.23	-8.76
SR7 $N_{jet} \geq 2$ $N_{bjet} \geq 2$ $H_T > 600$ $H_T^{miss} > 600$	79.97±3.21	76.04±6.57	87.22±0.78	8.31	12.82
SR8 $N_{jet} \geq 6$ $N_{bjet} \geq 2$ $H_T > 350$ $H_T^{miss} > 350$	92.61±3.46	97.6±7.44	96.21±0.8	3.74	-1.44
SR9 $N_{jet} \geq 4$ $N_{bjet} \geq 2$ $H_T > 600$ $H_T^{miss} > 600$	74.42±3.1	71.5±6.37	81.86±0.76	9.09	12.66
SR10 $N_{jet} \geq 8$ $N_{bjet} \geq 3$ $H_T > 300$ $H_T^{miss} > 300$	5.55±0.85	9.08±2.27	7.36±0.16	24.59	-23.37
SR11 $N_{jet} \geq 6$ $N_{bjet} \geq 1$ $H_T > 600$ $H_T^{miss} > 600$	81.9±3.25	72.63±6.42	88.82±0.8	7.79	18.23
SR12 $N_{jet} \geq 10$ $N_{bjet} \geq 3$ $H_T > 850$ $H_T^{miss} > 850$	0.13±0.13	0.0±0.0	0.19±0.03	31.58	100.0

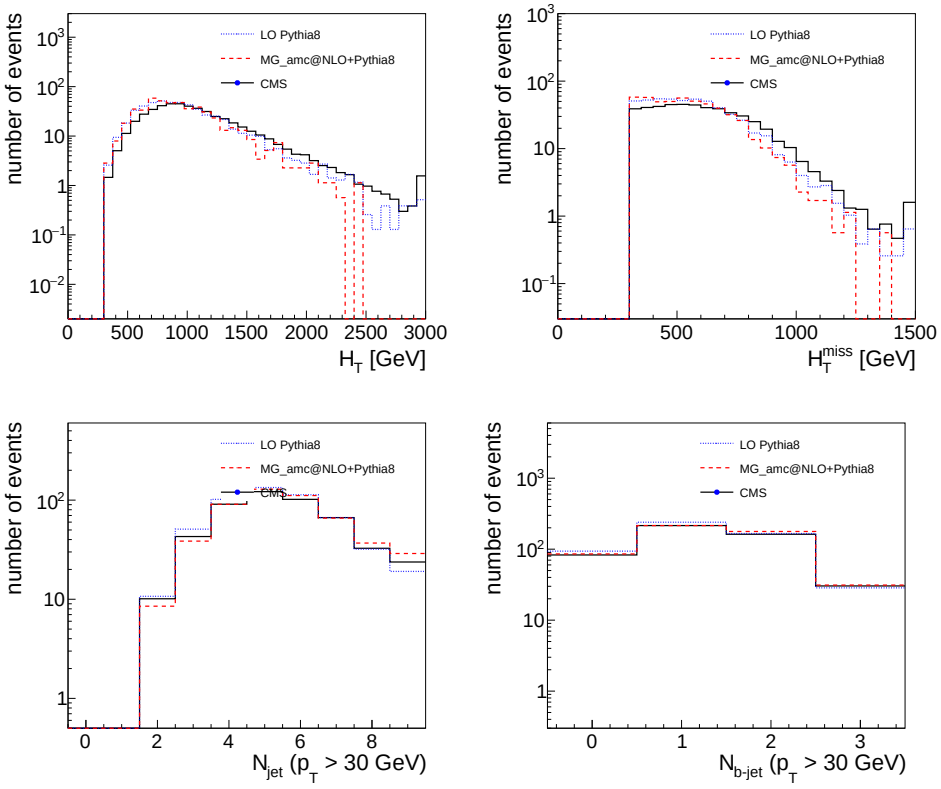

Fig. 14. Kinematic distributions for the T2tt-950-100 simplified model for the madanalysis5 implementation and those provided by CMS

Table 27. Pre-selection cutflow for the T2tt-600-400 simplified model.

Cut	MA5 Pythia8	MA5 Madgraph5 +Pythia8	CMS	MA5 Pythia8 diff [%]	MA5 Madgraph5 +Pythia8 diff [%]	MA5 Pythia8 drop [%]	MA5 Madgraph5 +Pythia8 drop [%]	CMS drop [%]
$N_{jet} \geq 2$	$99.5\pm^{0.1}_{0.1}$	$99.2\pm^{0.1}_{0.1}$	99.6±0.0	0.1	0.4	0.5	0.8	0.4
$H_T > 300$	$72.9\pm^{0.4}_{0.5}$	$67.4\pm^{0.4}_{0.4}$	72.2±0.3	-0.97	6.65	26.6	31.8	27.4
$H_T^{miss} > 300$	$12.9\pm^{0.3}_{0.3}$	$8.5\pm^{0.3}_{0.3}$	9.2±0.2	-40.22	7.61	60.0	58.9	63.0
$H_T > H_T^{miss}$	$12.8\pm^{0.3}_{0.3}$	$8.4\pm^{0.3}_{0.3}$	9.1±0.2	-40.66	7.69	0.1	0.1	0.1
NoIsoMuons	$10.5\pm^{0.3}_{0.3}$	$6.9\pm^{0.2}_{0.2}$	7.0±0.2	-50.0	1.43	2.3	1.5	2.1
NoMuonsTracks	$10.4\pm^{0.3}_{0.3}$	$6.8\pm^{0.2}_{0.2}$	6.9±0.2	-50.72	1.45	0.1	0.1	0.1
NoIsoElectrons	$8.5\pm^{0.3}_{0.3}$	$5.4\pm^{0.2}_{0.2}$	5.4±0.1	-57.41	0.0	1.9	1.4	1.5
NoElectronsTracks	$8.4\pm^{0.3}_{0.3}$	$5.3\pm^{0.2}_{0.2}$	5.2±0.1	-61.54	-1.92	0.1	0.1	0.2
NoIsoTracks	$8.1\pm^{0.3}_{0.3}$	$5.1\pm^{0.2}_{0.2}$	4.8±0.1	-68.75	-6.25	0.3	0.2	0.4
NoIsoPhotons	$8.0\pm^{0.3}_{0.3}$	$5.1\pm^{0.2}_{0.2}$	4.7±0.1	-70.21	-8.51	0.1	0.0	0.1
$\Delta\Phi_{H_T^{miss},j1} > 0.5$	$8.0\pm^{0.3}_{0.3}$	$5.1\pm^{0.2}_{0.2}$	4.7±0.1	-70.21	-8.51	0.0	0.0	0.0
$\Delta\Phi_{H_T^{miss},j2} > 0.5$	$7.3\pm^{0.3}_{0.3}$	$4.3\pm^{0.2}_{0.2}$	3.9±0.1	-87.18	-10.26	0.7	0.8	0.8
$\Delta\Phi_{H_T^{miss},j3} > 0.3$	$6.7\pm^{0.3}_{0.3}$	$3.7\pm^{0.2}_{0.2}$	3.4±0.1	-97.06	-8.82	0.6	0.6	0.5
$\Delta\Phi_{H_T^{miss},j4} > 0.3$	$6.2\pm^{0.3}_{0.2}$	$3.2\pm^{0.2}_{0.2}$	3.0±0.1	-106.67	-6.67	0.5	0.5	0.4

Table 28. Signal yield in the aggregated signal regions for the T2tt-600-400 simplified model.

Agg SR	MA5 Pythia8 yield	MA5 Madgraph5+Pythia8 yield	CMS yield	MA5 Pythia8 diff [%]	MA5 Madgraph5+Pythia8 diff [%]
SR1 $N_{jet} \geq 2$ $N_{bjet} = 0$ $H_T > 600$ $H_T^{miss} > 600$	16.01±6.54	8.75±4.37	7.51±0.53	-113.18	-16.51
SR2 $N_{jet} \geq 4$ $N_{bjet} = 0$ $H_T > 1700$ $H_T^{miss} > 850$	0.0±0.0	0.0±0.0	0.32±0.07	100.0	100.0
SR3 $N_{jet} \geq 6$ $N_{bjet} = 0$ $H_T > 600$ $H_T^{miss} > 600$	8.0±4.62	8.75±4.37	4.53±0.36	-76.6	-93.16
SR4 $N_{jet} \geq 8$ $N_{bjet} = 0-1$ $H_T > 600$ $H_T^{miss} > 600$	10.67±5.34	10.93±4.89	8.71±0.54	-22.5	-25.49
SR5 $N_{jet} \geq 10$ $N_{bjet} = 0-1$ $H_T > 1700$ $H_T^{miss} > 850$	0.0±0.0	0.0±0.0	0.23±0.07	100.0	100.0
SR6 $N_{jet} \geq 4$ $N_{bjet} \geq 2$ $H_T > 300$ $H_T^{miss} > 300$	544.29±38.11	325.77±26.69	254.99±3.37	-113.46	-27.76
SR7 $N_{jet} \geq 2$ $N_{bjet} \geq 2$ $H_T > 600$ $H_T^{miss} > 600$	32.02±9.24	26.24±7.57	19.85±0.92	-61.31	-32.19
SR8 $N_{jet} \geq 6$ $N_{bjet} \geq 2$ $H_T > 350$ $H_T^{miss} > 350$	232.12±24.89	161.79±18.81	130.96±2.34	-77.24	-23.54
SR9 $N_{jet} \geq 4$ $N_{bjet} \geq 2$ $H_T > 600$ $H_T^{miss} > 600$	32.02±9.24	26.24±7.57	19.67±0.91	-62.79	-33.4
SR10 $N_{jet} \geq 8$ $N_{bjet} \geq 3$ $H_T > 300$ $H_T^{miss} > 300$	21.34±7.55	28.42±7.88	20.36±0.71	-4.81	-39.59
SR11 $N_{jet} \geq 6$ $N_{bjet} \geq 1$ $H_T > 600$ $H_T^{miss} > 600$	80.04±14.61	59.03±11.36	30.97±1.16	-158.44	-90.6
SR12 $N_{jet} \geq 10$ $N_{bjet} \geq 3$ $H_T > 850$ $H_T^{miss} > 850$	2.67±2.67	0.0±0.0	0.09±0.03	-2866.67	100.0

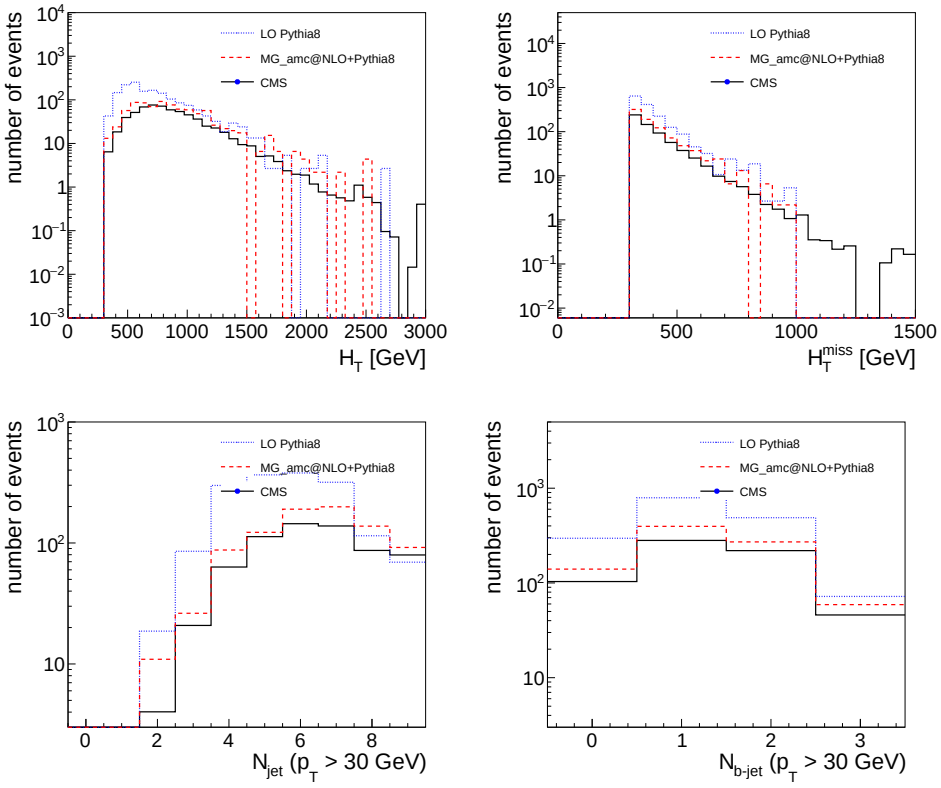

Fig. 15. Kinematic distributions for the T2tt-600-400 simplified model for the madanalysis5 implementation and those provided by CMS

4. Conclusions

We have presented a recast-ready implementation of *Search for supersymmetry in proton-proton collisions at 13 TeV in final states with jets and missing transverse momentum* (CMS-SUS-19-006).[1] The implementation has been validated using information made available by the CMS experiment/analysis team.[2]

We find that the accompanying code provides a good description of the signal acceptance of a wide range of simplified models of supersymmetry, where acceptances and distributions generally agree with official results to within 20%, or else within statistical uncertainties. We note that in a few cases this general statement does not apply. Most importantly, for the uncompressed T1qqqq model, there appears to be an inconsistency between the distributions provided by CMS and the aggregate signal region counts, which imply that the yield table is likely incorrectly reported. We have communicated this to the CMS analysis team and they agreed there is an issue that needs to be solved with the identified table. In the case of uncompressed bottom squark models, our implementation overestimates the signal yield in the highest bin of n_b of up to 40%, which we think is due to a lack of consistency between the `Delphes` implementation and that of the CMS simulation. We note that it is most robust to use a combination of signal regions in any interpretation, since a signal event that wrongfully migrates from one bin of n_b to another will be in this way be picked up by another signal region, and a comparable sensitivity will be retained. Other apparent differences appear to be consistent with statistical fluctuations in the yields.

Acknowledgments

Dedications and funding information may be included here.

References

1. A. M. Sirunyan *et al.* [CMS], JHEP **10** (2019), 244 doi:10.1007/JHEP10(2019)244 [arXiv:1908.04722 [hep-ex]].
2. Search for supersymmetry in proton-proton collisions at 13 TeV in final states with jets and missing transverse momentum , `http://cms-results.web.cern.ch/cms-results/public-results/publications/SUS-19-006/`, 13 08 2019.
3. E. Conte, B. Fuks and G. Serret, Comput. Phys. Commun. **184** (2013) 222 [arXiv:1206.1599 [hep-ph]].
4. E. Conte, B. Dumont, B. Fuks and C. Wymant, Eur. Phys. J. C **74** (2014) no.10, 3103 [arXiv:1405.3982 [hep-ph]].
5. B. Dumont *et al.*, Eur. Phys. J. C **75** (2015) no.2, 56 [arXiv:1407.3278 [hep-ph]].
6. E. Conte and B. Fuks, Int. J. Mod. Phys. A **33** (2018) no.28, 1830027 [arXiv:1808.00480 [hep-ph]].
7. Malte, Mrowietz and Bein, Sam and Sonneveld, Jory, "Re-implementation of a search for supersymmetry in the HT/missing HT channel (137 fb-1; CMS-SUSY-19-006)," Open Data @ UCLouvain, doi:10.14428/DVN/4DEJQM [arXiv:1908.04722 [hep-ex]] https://doi.org/10.14428/DVN/4DEJQM.

8. M. Cacciari, G. P. Salam and G. Soyez, JHEP **04** (2008), 063 doi:10.1088/1126-6708/2008/04/063 [arXiv:0802.1189 [hep-ph]].
9. R. Frederix, S. Frixione, V. Hirschi, D. Pagani, H. S. Shao and M. Zaro, JHEP **07** (2018), 185 doi:10.1007/JHEP07(2018)185 [arXiv:1804.10017 [hep-ph]].
10. C. Degrande, C. Duhr, B. Fuks, D. Grellscheid, O. Mattelaer and T. Reiter, Comput. Phys. Commun. **183** (2012), 1201-1214 doi:10.1016/j.cpc.2012.01.022 [arXiv:1108.2040 [hep-ph]].
11. C. Duhr and B. Fuks, Comput. Phys. Commun. **182** (2011), 2404-2426 doi:10.1016/j.cpc.2011.06.009 [arXiv:1102.4191 [hep-ph]].
12. R. D. Ball, V. Bertone, S. Carrazza, C. S. Deans, L. Del Debbio, S. Forte, A. Guffanti, N. P. Hartland, J. I. Latorre and J. Rojo, *et al.* Nucl. Phys. B **867** (2013), 244-289 doi:10.1016/j.nuclphysb.2012.10.003 [arXiv:1207.1303 [hep-ph]].
13. A. Buckley, J. Ferrando, S. Lloyd, K. Nordström, B. Page, M. Rüfenacht, M. Schönherr and G. Watt, Eur. Phys. J. C **75** (2015), 132 doi:10.1140/epjc/s10052-015-3318-8 [arXiv:1412.7420 [hep-ph]].
14. T. Sjostrand, S. Mrenna and P. Z. Skands, Comput. Phys. Commun. **178** (2008), 852-867 doi:10.1016/j.cpc.2008.01.036 [arXiv:0710.3820 [hep-ph]].
15. T. Sjöstrand, S. Ask, J. R. Christiansen, R. Corke, N. Desai, P. Ilten, S. Mrenna, S. Prestel, C. O. Rasmussen and P. Z. Skands, Comput. Phys. Commun. **191** (2015), 159-177 doi:10.1016/j.cpc.2015.01.024 [arXiv:1410.3012 [hep-ph]].
16. A. M. Sirunyan *et al.* [CMS], JINST **13** (2018) no.05, P05011 doi:10.1088/1748-0221/13/05/P05011 [arXiv:1712.07158 [physics.ins-det]].